International Journal of Network Dynamics and Intelligence Scilight

Article

Predefined Time Fuzzy Adaptive Control of Switched Fractional-Order Nonlinear Systems with Input Saturation

Lusong Ding and Weiwei Sun*

Institute of Automation, Qufu Normal University, Qufu 273165, China
* Correspondence: wwsun@hotmail.com

Received: 31 August 2023
Accepted: 31 October 2023
Published: 21 December 2023

Abstract: This article investigates the predefined-time fuzzy adaptive tracking control problem for a class of nonlinear switched fractional-order systems with input saturation and external disturbances under a nonstrict feedback structure. By combining the backstepping technique and the common Lyapunov function method, a predefined-time switching control method is constructed based on a novel fractional-order auxiliary function. The fuzzy logic system and the adaptive method are introduced to identify unknown compounded continuous functions. Moreover, the issue of calculating explosion and the problem of singularity are tackled through the newly proposed predefined-time and filter-based dynamic surface control. Especially, the construction of a continuous term in the controller eliminates possible chattering. The developed control strategy achieves that the closed-loop system is practically predefined-time stable under arbitrary switchings, where the upper bound of the settling-time can be defined by users in advance. Finally, two simulation examples are illustrated to prove the feasibility and effectiveness of the presented scheme.

Keywords: adaptive control; fractional-order systems; predefined-time control; input saturation; switched system

1. Introduction

Over the past decades, fractional-order systems have been widely studied in practical industrial areas, such as engineering, physics, biology, and chemistry. The fractional-order systems can depict and reflect the properties of objects more truly and accurately than the integer-order systems, thereby obtaining better control performance. Theoretical and practical research on fractional-order system control has attracted considerable interests, and different control approaches have been successfully applied including the sliding-mode control methods, robust control methods and adaptive control methods [1−3].

Owing to their strong learning and approximation abilities, fuzzy logic systems (FLSs) and neural networks (NNs) have been extensively used in the adaptive control of nonlinear systems to cope with dynamic uncertainties. The control performance of fractional-order systems has been improved by combining several advanced control methods. In [4] and [5], a robust adaptive control scheme was proposed for single-input single-output (SISO) fractional-order nonlinear systems by adopting the backstepping control technique. Such a scheme was extended in [6−8] to study multi-input multi-output (MIMO) fractional-order nonlinear systems. Considering the input nonlinearity and immeasurable states, the observer-based output feedback control scheme was presented in [6] for fractional-order nonlinear systems based on the fractional adaptive type-2 fuzzy technique. The adaptive decentralized control was investigated in [7] for nonlinear interconnected systems with mismatched interconnections. Furthermore, the fully distributed adaptive consensus tracking algorithm was proposed in [8] for nonlinear fractional-order multiagent systems subject to heterogeneous uncertainties.

In a variety of application scenarios, the input saturation is a commonly occurring nonlinearity and is considered to be a major threat to the control system [9−11]. The input saturation may be caused by the physical limitation of the actuator itself, or may be artificially introduced to prevent the excessive impact from destroying the stability of the actuator or even the system. Therefore, designing a suitable control approach for nonlinear systems with input saturation is an essential and necessary issue. By far, there have been two ways to handle the input saturation which include introducing an auxiliary system to the controller [12] or considering the presence of the saturation in the sys-

tem [13]. Accordingly, the constraint control approach was designed in [14] for nonlinear fractional-order systems by considering the effect of the input saturation and state constraints whose extension to the nontriangular nonlinear systems was presented in [15]. Furthermore, an event-triggered control strategy was proposed in [16] which can dynamically adjust the threshold parameters according to the system output, thereby reducing the communication burden. Note that the above research work all focuses on nonswitched fractional-order systems.

It is generally known that the switched system, as a kind of hybrid system, is composed of exact switching rules and a series of switching subsystems, and has found widespread applications based on different controller switching strategies [17, 18]. Control schemes designed for switched systems are significant and challenging in various engineering control sytems, such as hybrid vehicle systems, robot control systems, and switching power converters [19, 20]. In [21], the common Lyapunov function approach was applied to solve the problem of global stabilization for arbitrary switching systems. The neuro-adaptive control method was proposed in [22] for switching nonlinear systems via the average dwell-time technique, and this method was successfully generalized to nonlinear switching fractional-order systems [23−25]. Nevertheless, the aforementioned work has focused relatively less on the time optimization problem of the control systems.

Generally, the actual system should be quickly stabilized to a stable operating region within a prescribed time in case of disturbances or uncertainties. Owing to its characteristics of fast response and disturbance rejection [26], the finite-time control strategy is suitable for keeping the control performance of nonlinear systems, and fruitful results have been obtained on the study of finite-time convergence [27, 28]. Note that the upper limited convergence time of the system is a bounded function depending on the initial values [29]. For many practical systems, the initial condition cannot be set arbitrarily to suit the actual needs, which limits the implementation of finite-time control. This motivates the study on fixed-time stability where the settling-time is independent of the initial value [30−32]. A noteworthy point is that both finite-time control and fixed-time control ignore the direct correlation between the bound of the convergence time and the designed system parameters, making it relatively challenging to search for parameters that satisfy the requirement of the convergence time.

To effectively reduce conservatism and easily adjust the convergence time bound, some researchers investigated the predefined-time Lyapunov stability [33−35] and developed practical predefined-time convergent adaptive control schemes for nonlinear systems [36−39]. Such a method further develops the predefined-time control theory. Among them, the adaptive predefined-time control scheme was designed in [36, 37] for nonlinear systems with the convergence time and tracking accuracy set artificially in advance. Furthermore, the new predefined-time filters were designed in [38, 39] to avoid problems of "explosion of complexity" and singularity. The predefined time control has the merit that the settling-time is determined only by the adjustment parameters relative to the finite/fixed time control, which means that the settling-time can be directly specified by adjusting the predefined time parameters. This attractive feature promotes the applications of predefined time control in a wide range of fields, such as tailless aircrafts [39], autonomous surface vehicles [40], and rigid spacecrafts [41]. Besides, a robust controller was designed in [42−44] with predefined-time convergence for fractional-order nonlinear systems, whereas the uncertainties and nonlinearities were not considered. So far, the predefined-time control has not attracted full attention for fractional-order nonlinear systems subject to input nonlinearities including input saturation, asymmetric time-varying constraints, and unknown control directions.

Motivated by the foregoing discussions, this study investigates a new predefined-time control scheme for uncertain MIMO switched fractional-order nonlinear systems with input saturation and external disturbances. Compared with the previous literature, the main contributions are given as follows.

1) In this paper, a novel fractional-order predefined-time control scheme is first developed based on an auxiliary function in a unified framework, where the convergence time explicitly appears as a tuning parameter. This scheme is applied to solve the tracking control problem for a class of switched fractional-order nonlinear systems, while the existing methods in [36−39, 42, 43] are not directly applicable to tackle the considered problem.

2) The presented fuzzy adaptive control scheme guarantees the control performance of closed-loop systems when arbitrary switching and input saturation happen, making it more generalized than the schemes in [6−8, 15, 16, 22].

3) An improved filtering technique is adopted to overcome the effect of repeated derivatives in the backstepping and singularity problems. Note that the chattering phenomenon may arise in the results of [36−39].

2. Problem Formulation and Preliminaries

2.1. Preliminaries

Definition 1. [45] *For a real function $f(t)$, the Riemann-Liouville (RL) fractional integral with fractional-order $\alpha \in \mathbb{R}^+$ is defined as follows:*

$$\mathcal{I}_t^{\alpha} f(t) = \frac{1}{\Gamma(\alpha)} \int_0^t (t-\tau)^{\alpha-1} f(\tau) d\tau \tag{1}$$

where $\Gamma(\cdot) = \int_0^{+\infty} \tau^{\alpha-1} e^{-\tau} d\tau$ *denotes the Gamma function.*

Definition 2. [45] *The Caputo* α*-order fractional derivative for* $f(t) \in C^n([t_0, +\infty], \mathbb{R})$ *can be written as*

$$ {}_0^C\mathcal{D}_t^{\alpha} f(t) = \frac{1}{\Gamma(n-\alpha)} \int_0^t (t-\tau)^{n-\alpha-1} f^{(n)}(\tau) d\tau, \tag{2}$$

where ${}_0^C\mathcal{D}_t^{\alpha}$ *represents the* α*th order Caputo differential operator,* $n-1 < \alpha < n$ *and* $n \in \mathbb{N}^+$*. This paper only considers the case of* $\alpha \in (0,1)$ *and* $n = 1$*.*

Property 1. [46] *Assume that the Caputo fractional derivative* ${}_0^C\mathcal{D}_t^{\alpha} f(t)$ *with* $n-1 \leqslant \alpha < n$ *is integrable, then*

$$\mathcal{I}_t^{\alpha}\, {}_0^C\mathcal{D}_t^{\alpha} f(t) = f(t) - \sum_{k=0}^{n-1} \frac{f^{(k)}(0)}{k!} t^k. \tag{3}$$

Particularly, if $\alpha \in (0,1)$*, one has* $\mathcal{I}_t^{\alpha}\, {}_0^C\mathcal{D}_t^{\alpha} f(t) = f(t) - f(0)$*.*

Lemma 1. [47] *Suppose that* $x(t) \in \mathbb{R}^n$ *is a smooth and differentiable function vector, then* ${}_0^C D_t^{\alpha}(x^T(t)x(t)) \leqslant 2x^T(t)\, {}_0^C D_t^{\alpha} x(t)$ *for* $\forall t \geqslant t_0$*.*

Lemma 2. [4] *For* $x \in \mathbb{R}$ *and a positive constant* ϵ*, one has*

$$0 \leqslant |x| - \frac{x^2}{\sqrt{x^2+\epsilon^2}} \leqslant \epsilon.$$

Lemma 3. [31] *For any positive constants* $\kappa_1, \kappa_2, \kappa_3$*, the following inequality holds:*

$$|x|^{\kappa_1} |y|^{\kappa_2} \leqslant \frac{\kappa_1}{\kappa_1+\kappa_2} \kappa_3 |x|^{\kappa_1+\kappa_2} + \frac{\kappa_1}{\kappa_1+\kappa_2} \kappa_3^{-\frac{\kappa_1}{\kappa_2}} |y|^{\kappa_1+\kappa_2}.$$

Lemma 4. [31] *For* $y \geqslant x$ *and* $\mu > 1$*, the following inequality holds:*

$$x(y-x)^{\mu} \leqslant \frac{\mu}{1+\mu} (y^{1+\mu} - x^{1+\mu}).$$

Lemma 5. [31] *For a constant* q *with* $0 < q \leqslant 1$ *and* $x_i \in \mathbb{R}$*, the following inequality holds:*

$$\left(\sum_{i=1}^n |x_i| \right)^q \leqslant \sum_{i=1}^n |x_i|^q \leqslant n^{1-q} \left(\sum_{i=1}^n |x_i| \right)^q.$$

In the subsequently developed control design scheme, a fuzzy-approximation based approach is employed to approximate the continuous function. Note that FLSs have the following universal approximation property.

Lemma 6. [48] *Suppose that* $f(x)$ *is a continuous arbitrary function defined in a compact set* Ω*. For any small positive scalar* ε*,*

$$\sup_{x \in \Omega} |f(x) - \theta^{*T} \varphi(x)| \leqslant \delta,\ |\delta| \leqslant \varepsilon, \tag{4}$$

holds where θ^{*T} *denotes the ideal constant weights,* $\varphi(x) = [\varphi_1(x), \varphi_2(x), \cdots, \varphi_s(x)]^T$ *is the basis function vector with* $s > 1$ *representing the number of the fuzzy rules, and* δ *is the fuzzy minimum approximation error.*

2.2. Predefined Time Stability Theory

Consider the integer-order system:

$$\dot{x}(t) = f(t, x, d),\ x(0) = x_0, \tag{5}$$

where $x \in \mathbb{R}^n$ represents the system states, $d \in \mathbb{R}^n$ denotes the unknown but bounded disturbances, and $f(x,t): \mathbb{R}^n \to \mathbb{R}^n$ stands for the nonlinear function. We assume that the origin is the equilibrium point of system (5).

Definition 3. [33, 34] *For nonlinear system (5), the equilibrium point* $x = 0$ *is fixed-time convergent if it is finite-time stable and there exists a bounded setting-time function* $T(x_0) < \infty$ *such that* $T(x_0)$ *is bounded for* $t \geqslant T(x_0)$*. If there exists a predefined time constant* T_d *satisfying* $T(x_0) \leqslant T_d$*, then the origin of system (5) is predefined-time stable.*

Lemma 7. [34] *For dynamical system (5), if there exists a continuous and differentiable positive-definite function* $V(x)$ *such that*

$$\dot{V}(x) \leqslant -\frac{\pi}{\varrho T_d} (V^{1+\frac{\varrho}{2}} + V^{1-\frac{\varrho}{2}}), \tag{6}$$

where $\varrho \in (0,1)$*, and* T_d *is the setting time. Then, the trajectory of system (5) is predefined-time stable.*

Theorem 1. *For system (5), suppose that there exists a scalar function* $V(x)$ *such that*

$$\dot{V}(x) \leqslant -\frac{\pi}{\varrho T_d}(aV^{1+\frac{\varrho}{2}} + bV^{1-\frac{\varrho}{2}}) + c, \tag{7}$$

where $\varrho \in (0,1)$*.* $a > 0$*,* $b > 0$ *and* $c > 0$ *are the condition parameters for the convergence of the system. Then, the origin of system (5) is practically predefined-time stable. Besides, the solution* $x(t, x_0)$ *is bounded by*

$$x \in \left\{ V(x) : V(x) \leqslant \min\left\{ \left(\frac{2c\varrho T_d}{\pi b}\right)^{\frac{2}{2-\varrho}}, \left(\frac{2c\varrho T_d}{\pi a}\right)^{\frac{2}{2+\varrho}} \right\} \right\}, \tag{8}$$

where T_p *is the settling-time satisfying* $T_p < T_{\max} = \sqrt{2}T_d/\sqrt{ab}$ *with* $T_{\max}$ *being the upper bound.*

Proof 1. *Now, consider the following two parts.*

i) Inequality (7) implies

$$\dot{V}(x) \leqslant -\frac{\pi}{2\varrho T_d} aV^{1+\frac{\varrho}{2}} - \frac{\pi}{2\varrho T_d} aV^{1+\frac{\varrho}{2}} - \frac{\pi}{\varrho T_d} bV^{1-\frac{\varrho}{2}} + c. \tag{9}$$

(9) can be rewritten as

$$\dot{V}(x) \leqslant -\frac{\pi}{2\varrho T_d} aV^{1+\frac{\varrho}{2}} - \frac{\pi}{\varrho T_d} bV^{1-\frac{\varrho}{2}} \tag{10}$$

for $V(x) \geqslant \left(\frac{2\varrho T_d c}{\pi a}\right)^{\frac{2}{2+\varrho}}$*. According to Lemma 7, it is obtained that system (5) is predefined-time stable with* $t \to T_p$*, and the state trajectory* $x(x_0, t)$ *is bounded by* $\left\{V(x) \leqslant \left(\frac{2\varrho T_d c}{\pi a}\right)^{\frac{2}{2+\varrho}}\right\}$*.*

Integrating (10) over [0, T_p*], one has*

$$\int_0^{T_p} \frac{\dot{V}dt}{\frac{a}{2}V^{1+\frac{\varrho}{2}} + bV^{1-\frac{\varrho}{2}}} \leqslant -\int_0^{T_p} \frac{\pi}{\varrho T_d} dt, \tag{11}$$

which is followed by

$$\begin{aligned} T_p &\leqslant -\frac{\varrho T_d}{\pi} \int_{V(x_0)}^{V(x_1)} \frac{dV}{\frac{a}{2}V^{1+\frac{\varrho}{2}} + bV^{1-\frac{\varrho}{2}}} \\ &= -\frac{2\sqrt{2}T_d}{\pi\sqrt{ab}} \int_{V(x_0)}^{V(x_1)} \frac{d(\sqrt{\frac{a}{2b}}V^{\frac{\varrho}{2}})}{1 + \frac{a}{2b}V^{\varrho}} \\ &\leqslant \frac{\sqrt{2}T_d}{\sqrt{ab}} \left[\frac{2}{\pi}\arctan\left(\sqrt{\frac{a}{2b}}V^{\frac{\varrho}{2}}(x_0)\right)\right] \\ &\leqslant \frac{\sqrt{2}T_d}{\sqrt{ab}}, \end{aligned} \tag{12}$$

where x_0 *is the initial state during* $t = 0$ *and* x_1 *is the state when the system is stable during* $t = T_p$*. Thus, the upper-bound settling time is given by* $T_p < T_{\max} = \sqrt{2}T_d/\sqrt{ab}$*.*

ii) It follows from (7) that

$$\dot{V}(x) \leqslant -\frac{\pi}{\varrho T_d} aV^{1+\frac{\varrho}{2}} - \frac{\pi}{2\varrho T_d} bV^{1-\frac{\varrho}{2}} - \frac{\pi}{2\varrho T_d} bV^{1-\frac{\varrho}{2}} + c. \tag{13}$$

Similar to the previous proof, we know that the formula for calculating the convergence region is $\left\{V(x) \leqslant \left(\frac{2\varrho T_d c}{\pi b)}\right)^{\frac{2}{2-\varrho}}\right\}$ *with* $t \to T_p < T_{\max} = \sqrt{2}T_d/\sqrt{ab}$*, which completes this proof.*

Remark 1. *In Lemma 1, there exist two adjustable parameters a and bwhich makes the condition generally available for the actual system. Note that when* $a = b = 1$ *and* $c = 0$*, the result in [34] is a particular case of Lemma 7. Thus, the existence of adjustable parameters a and b provides greater flexibility to the controller design than the fixed case of a=b=1. Further, the values of a and b are the minimum gains of the controller. Compared with the results proposed in [39], the convergence time and convergence region of the system are much easier to be adjusted. Thus, the proposed scheme is suitable for wider application areas.*

Remark 2. *Note that Theorem 1 is a generalized form of Lemma 7 for the predefined time stability of integer-order systems. Due to the difference between integer-order calculus and fractional-order calculus, the results of predefined time stability of integer-order systems cannot be directly applied to fractional-order systems. Therefore, a novel frac-*

tional-order auxiliary function (20) is designed to solve this problem and guarantee the predefined-time stability of Caputo fractional-order systems.

Next, consider the following definition of the predefined-time convergence for fractional-order systems.

Definition 4. *[42,43] Suppose that there is a fractional-order nonlinear system* ${}_0^C\mathcal{D}_t^\alpha x(t) = f(t, x(t))$*, where* $x \in \mathbb{R}^n$ *is the system state, and* $f(t, x(t))$ *is a continuous function with* $\alpha \in (0,1)$*. Then, the solution will converge to* $\check{x} \in \mathbb{R}^n$ *with the predefined-time* $T_d > 0$*, if* $\lim_{t \to T_d} x(t) = \check{x}$ *and* $x(t) = \check{x}$ *hold for* $\forall t \geqslant T_d$*, where* T_d *can be preassigned.*

2.3. System Description

Consider a class of nonlinear nonstrict-feedback MIMO fractional-order switched systems composed of M subsystems. The ith ($i = 1, 2, \cdots, M$) subsystem is expressed by

$$\begin{aligned} {}_0^C\mathcal{D}_t^\alpha x_{i,j_i} &= x_{i,j_i+1} + f_{i,j_i}^{[\sigma(t)]}(x) + d_{i,j_i}^{[\sigma(t)]}(t) \\ {}_0^C\mathcal{D}_t^\alpha x_{i,n_i} &= u_i(v_i(t)) + f_{i,n_i}^{[\sigma(t)]}(x) + d_{i,n_i}^{[\sigma(t)]}(t) \\ y_i &= x_{i,1} \end{aligned} \tag{14}$$

where $x = [x_1^T, x_2^T, \cdots, x_M^T]^T \in \mathbb{R}^{M \times n_i}$ ($x_i = [x_{i,1}, x_{i,2}, \cdots, x_{i,n_i}]^T \in \mathbb{R}^{n_i}$) is the system state variable, and $y_i \in \mathbb{R}$ is the system output variable. $\sigma(t) : [0, \infty) \to \Xi = \{1, 2, \cdots, N\}$ stands for the switching signal with N being the number of the subsystems, which is assumed to be a known piecewise continuous (from the right) function with respect to the time. When $[\sigma(t)] = [p]$ and $[p] \in \Xi$, it means that the pth subsystem is activated. $f_{i,j_i}^{[\sigma(t)]}(x_i) \in \mathbb{R}$ denotes an unknown smooth nonlinear function. $d_{i,j_i}^{[\sigma(t)]}(t) \in \mathbb{R}$ denotes the unknown but bounded external disturbance which is bounded by $|d_{i,j_i}^{[\sigma(t)]}(t)| \leqslant \bar{d}_{i,j_i}^{[\sigma(t)]}$, where $\bar{d}_{i,j_i}^{[\sigma(t)]}$ is an unknown constant ($i = 1, 2, \cdots, M$, $j_i = 1, 2, \cdots, n_i$).

Besides, v_i is the input signal of the controller. $u_i(v_i)$ is the nonlinear saturation input of the ith subsystem, which is the output of the saturation nonlinearity described as follows [12]:

$$u_i(v_i) = \mathrm{sat}(v_i) = \begin{cases} \bar{u}_i, & v_i \geqslant \bar{u}_i, \\ v_i, & \underline{u}_i < v_i < \bar{u}_i, \\ \underline{u}_i, & v_i \leqslant \underline{u}_i, \end{cases} \tag{15}$$

where $\underline{u}_i < 0$ and $\bar{u}_i > 0$ are bounds of $u_i(v_i)$. To deal with non-tiny at sharp corners, a smooth hyperbolic tangent function $m_i(v_i)$ of the ith system is denoted as follows:

$$m_i(v_i) = \begin{cases} \bar{u}_i \cdot \tanh\left(\dfrac{v_i}{\bar{u}_i}\right), & v_i \geqslant 0 \\ \underline{u}_i \cdot \tanh\left(\dfrac{v_i}{\underline{u}_i}\right), & v_i < 0 \end{cases} \tag{16}$$

Accordingly, $\mathrm{sat}(v_i)$ in (15) can be decomposed as

$$\mathrm{sat}(v_i) = m_i(v_i) + h_i(v_i), \tag{17}$$

where $|h_i(v_i)| = |\mathrm{sat}(v_i) - m_i(v_i)| \leqslant \max\{\underline{u}_i(\tanh(1) - 1), \bar{u}_i(1 - \tanh(1))\} = H_i$. By the mean-value theorem, we can get $m_i(v_i) = m_{v_{i,\mu_i}}(v_i - v_{i,0}) + h_i(v_{i,0})$, $m_{v_{i,\mu_i}} = (\partial m(v_i)/\partial v_i)|_{v_i = v_{\mu_i}}$ and $v_{\mu_i} = \mu_i + (1 - \mu_i)v_{i,0}$ with $0 < \mu_i < 1$.

By choosing $v_{i,0} = 0$, we have

$$u_i(v_i) = \mathrm{sat}(v_i) = m_{v_{i,\mu_i}} v_i + h_i(v_i), \tag{18}$$

where $0 < m_{i,b} \leqslant |m_{v_{i,\mu_i}}| \leqslant 1$ and $m_{i,b}$ is an unknown positive constant.

To design the adaptive tracking scheme for system (14), the following two common assumptions are required.

Assumption 1. *For* $i = 1, 2, ..., M$*, the reference signal* $y_{i,d}$ *and its* α*-order time-derivatives are continuous and bounded, i.e.,* $y_{i,d}^2 + ({}_0^C\mathcal{D}_t^\alpha y_{i,d})^2 + ({}_0^C\mathcal{D}_t^\alpha [{}_0^C\mathcal{D}_t^\alpha y_{i,d}])^2 \leqslant \bar{y}_i$*, where* $\bar{y}_i$ *is a positive constant.*

Control objective: we will design a practically predefined-time tracking control scheme for system (14) without violation of input saturation such that 1) the reference signal can be tracked by the system output in a predefined time and 2) all the closed-loop signals remain bounded.

3. Main Results

3.1. Controller Design

In this subsection, on account of the backstepping technology, the adaptive fuzzy predefined-time controller of system (14) is constructed for the pth activated subsystem.

For $i = 1, \cdots, M$ and $j_i = 2, \cdots, n_i$, define the following coordinates transformation:

$$z_{i,1} = x_{i,1} - y_{i,d}$$
$$z_{i,j_i} = x_{i,j_i} - \hat{\alpha}_{i,j_i}, \tag{19}$$

where $y_{i,d}$ is a reference signal, and $\hat{\alpha}_{i,j_i}$ is the output of the first-order filter in connection with the virtual controller α_{i,j_i}. The filtering error is defined by $\nu_{i,j_i} = \hat{\alpha}_{i,j_i} - \alpha_{i,j_i}$.

Besides, we introduce the following novel auxiliary function:

$$\Psi_{i,j_i}(z_{i,j_i}) = \mathcal{I}_t^{1-\alpha} z_{i,j_i} + \mathcal{I}_t^{2-\alpha}\left(\frac{\pi}{\varrho T_d} z_{i,j_i}^{1+\frac{\varrho}{2}} + \frac{\pi}{\varrho T_d} z_{i,j_i}^{1-\frac{\varrho}{2}}\right), \tag{20}$$

where $i = 1,2,\cdots,M$ and $j_i = 1,2,\cdots,n_i$. $T_d > 0$ is a predefined parameter, and ϱ the ratio of two positive odd integers satisfying $\varrho > 0$, which implies that $1 + \varrho/2 > 1$ and $1 - \varrho/2 < 1$. Note that we assume the existence of a nonlinear function $\zeta_{i,j_i}(\Psi_{i,j_i})$ such that there exist strict positive constants ϖ_{i,j_i} satisfying $\Psi_{i,j_i}\zeta_{i,j_i}(\Psi_{i,j_i}) > \varpi_{i,j_i}|\Psi_{i,j_i}| > 0$ and $\varpi_{i,j_i} > |z_{i,j_i+1}|_{\max}$ $(i = 1,2,\cdots,M,\ j_i = 1,2,\cdots,n_i - 1)$. Then, we can deduce that the virtual control function α_{i,j_i} for $j_i = 1,2,\cdots,n_i$ is

$$\begin{aligned}\alpha_{i,j_i} = &-c_{i,j_i}\frac{\lambda\pi}{\varrho T_d}\Psi_{i,j_i}^{1+\varrho} - \omega_{i,j_i}\frac{\bar{\lambda}\pi\Psi_{i,j_i}^{3-2\varrho}}{\varrho T_d\sqrt{\Psi_{i,j_i}^{4-2\varrho} + \varsigma_{\Psi_i}^2}} - \frac{\pi}{\varrho T_d}\mathcal{I}_t^{1-\alpha}\left(z_{i,j_i}^{1+\frac{\varrho}{2}} + z_{i,j_i}^{1-\frac{\varrho}{2}}\right)\\ &+ {}_0^C\mathcal{D}_t^{\alpha}\bar{\alpha}_{i,j_i} - \zeta_{i,j_i}(\Psi_{i,j_i}) - \psi_{i,j_i}^{[p]}\Psi_{i,j_i}\hat{\Theta}_{i,j_i}^{[p]} - \hat{\rho}_{i,j_i}^{[p]}\tanh\left(\frac{\Psi_{i,j_i}}{\varsigma_{\rho_i}}\right),\ j_i = 1,\cdots,n_i - 1\end{aligned} \tag{21}$$

$$\begin{aligned}\alpha_{i,n_i} = \nu_i = &-c_{i,n_i}\frac{\lambda\pi}{\varrho T_d}\Psi_{i,n_i}^{1+\varrho} - \omega_{i,n_i}\frac{\bar{\lambda}\pi\Psi_{i,n_i}^{3-2\varrho}}{\varrho T_d\sqrt{\Psi_{i,n_i}^{4-2\varrho} + \varsigma_{\Psi_i}^2}} - \frac{\pi}{\varrho T_d}\mathcal{I}_t^{1-\alpha}\left(z_{i,n_i}^{1+\frac{\varrho}{2}} + z_{i,n_i}^{1-\frac{\varrho}{2}}\right)\\ &+ {}_0^C\mathcal{D}_t^{\alpha}\bar{\alpha}_{i,n_i} - \frac{\Psi_{i,n_i}}{2} - \psi_{i,n_i}^{[p]}\Psi_{i,n_i}\hat{\Theta}_{i,n_i}^{[p]} - \hat{\rho}_{i,n_i}^{[p]}\tanh\left(\frac{\Psi_{i,n_i}}{\varsigma_{\rho_i}}\right),\end{aligned} \tag{22}$$

where ${}_0^C\mathcal{D}_t^{\alpha}\bar{\alpha}_{i,1} = {}_0^C\mathcal{D}_t^{\alpha}y_{i,d}$. $c_{i,j_i} > 0$ and $\omega_{i,j_i} > 0$ for $j_i = 1,2,\cdots,n_i$. ς_{Ψ_i} and ς_{ρ_i} are the design constants. $\lambda = [(4n_i + 1)M)]^{\varrho/2}/2^{1+\varrho/2}$ and $\bar{\lambda} = 1/2^{1-\varrho/2}$. Other parameters will be defined later.

Step 1: When $\sigma(t) = p$, according to (14) and (19), one can obtain the derivative of $\Psi_{i,1}$ as

$$\dot{\Psi}_{i,1} = {}_0^{RL}\mathcal{D}_t^{\alpha}z_{i,1} + \mathcal{I}_t^{1-\alpha}\left(\frac{\pi}{\varrho T_d} z_{i,1}^{1+\frac{\varrho}{2}} + \frac{\pi}{\varrho T_d} z_{i,1}^{1-\frac{\varrho}{2}}\right) \tag{23}$$

Putting ${}_0^{RL}\mathcal{D}_t^{\alpha}(z_{i,1})$ into ${}_0^C\mathcal{D}_t^{\alpha}(z_{i,1})$ and substituting the error dynamics (19) into (23), one has

$$\begin{aligned}\dot{\Psi}_{i,1} = &\frac{z_{i,1}(0)}{\Gamma(1-\alpha)t^{\alpha}} + z_{i,2} + \nu_{i,2} + \alpha_{i,1} + f_{i,1}^{[p]}(x) + d_{i,1}^{[p]}(t)\\ &- {}_0^C\mathcal{D}_t^{\alpha}y_{i,d} + \mathcal{I}_t^{1-\alpha}\left(\frac{\pi}{\varrho T_d} z_{i,1}^{1+\frac{\varrho}{2}} + \frac{\pi}{\varrho T_d} z_{i,1}^{1-\frac{\varrho}{2}}\right),\end{aligned} \tag{24}$$

The candidate Lyapunov function is selected as

$$V_1 = \sum_{i=1}^{M}\left(\frac{1}{2}\Psi_{i,1}^2 + \frac{1}{2\gamma_{i,1}}\tilde{\Theta}_{i,1}^{[p]2} + \frac{1}{2\Gamma_{i,1}}\tilde{\rho}_{i,1}^{[p]2}\right), \tag{25}$$

where $\gamma_{i,1}$ and $\Gamma_{i,1}$ are positive design parameters. $\tilde{\Theta}_{i,1}^{[p]} = \Theta_{i,1}^{[p]*} - \hat{\Theta}_{i,1}^{[p]}$ is the parameter estimation error. $\hat{\Theta}_{i,1}^{[p]}$ is the estimate of $\Theta_{i,1}^{[p]*}$. Define $\tilde{\rho}_{i,1}^{[p]} = \rho_{i,1}^{[p]*} - \hat{\rho}_{i,1}^{[p]}$ as the parameter error with $\hat{\rho}_{i,1}^{[p]}$ being the estimate of $\rho_{i,1}^{[p]*}$. Among them, $\Theta_{i,1}^{[p]*} = \max\{\|\theta_{i,1}^{[p]*}\|^2\}$ and $\rho_{i,1}^{[p]*} = \delta_{i,1}^{[p]} + \bar{d}_{i,1}^{[p]}$.

By Lemma 6, an FLS $\theta_{i,1}^{[p]*T}\varphi_{i,1}^{[p]}(x)$ is used to approximate $\mathfrak{F}_{i,1}(x) = f_{i,1}^{[p]}(x) + z_{i,1}(0)/(\Gamma(1-\alpha)t^{\alpha})$. Based on (23) and Lemma 1, the time derivative of $V_{i,1}$ can be calculated as

$$\begin{aligned}\dot{V}_1 = \sum_{i=1}^{M}\Big[&\Psi_{i,1}(z_{i,2} + \nu_{i,2} + \alpha_{i,1} + \theta_{i,1}^{[p]*T}\varphi_{i,1}^{[p]}(x) + \delta_{i,1}^{[p]} + d_{i,1}^{[p]}(t) - {}_0^C\mathcal{D}_t^{\alpha}y_{i,d})\\ &- \frac{1}{\gamma_{i,1}}\tilde{\Theta}_{i,1}^{[p]}\dot{\hat{\Theta}}_{i,1}^{[p]} - \frac{1}{\Gamma_{i,1}}\tilde{\rho}_{i,1}^{[p]}\dot{\hat{\rho}}_{i,1}^{[p]} + \mathcal{I}_t^{1-\alpha}\left(\frac{\pi}{\varrho T_d} z_{i,1}^{1+\frac{\varrho}{2}} + \frac{\pi}{\varrho T_d} z_{i,1}^{1-\frac{\varrho}{2}}\right)\Big].\end{aligned} \tag{26}$$

By means of Young's inequality and the property of the fuzzy basis function $0 < \varphi_{i,1}^{[p]T}(x_{i,1})\varphi_{i,1}^{[p]}(x_{i,1}) \leqslant 1$, one has that

$$\begin{aligned}&\Psi_{i,1}[\theta_{i,1}^{[p]*T}\varphi_{i,1}^{[p]}(x)+\varepsilon_{i,1}^{[p]}+\bar{d}_{i,1}^{[p]}]\\&\leqslant|\Psi_{i,1}|\rho_{i,1}^{[p]*}+\frac{\|\theta_{i,1}^{[p]*}\|^2\Psi_{i,1}^2}{4\kappa_{i,1}\varphi_{i,1}^{[p]T}(x_{i,1})\varphi_{i,1}^{[p]}(x_{i,1})}+\kappa_{i,1}\varphi_{i,1}^{[p]T}(x_{i,1})\varphi_{i,1}^{[p]}(x_{i,1})\\&\leqslant\psi_{i,1}^{[p]}\Theta_{i,1}^{[p]*}\Psi_{i,1}^2+|\Psi_{i,1}|\rho_{i,1}^{[p]*}+\kappa_{i,1},\end{aligned}\tag{27}$$

where $\psi_{i,1}^{[p]}=1/(4\kappa_{i,1}\varphi_{i,1}^{[p]T}(x_{i,1})\varphi_{i,1}^{[p]}(x_{i,1}))$ and $\kappa_{i,1}$ are positive constants to be designed.

Substituting (27) into (26) yields

$$\begin{aligned}\dot{V}_1\leqslant\sum_{i=1}^{M}\Big[&\Psi_{i,1}(z_{i,2}+\alpha_{i,1}-{}_0^C\mathcal{D}_t^{\alpha}y_{i,d})+\psi_{i,1}^{[p]}\Theta_{i,1}^{[p]*}\Psi_{i,1}^2+\kappa_{i,1}\\&+|\Psi_{i,1}|\rho_{i,1}^{[p]*}-\frac{1}{\gamma_{i,1}}\tilde{\Theta}_{i,1}^{[p]}\dot{\hat{\Theta}}_{i,1}^{[p]}-\frac{1}{\Gamma_{i,1}}\tilde{\rho}_{i,1}^{[p]}\dot{\hat{\rho}}_{i,1}^{[p]}\Big].\end{aligned}\tag{28}$$

The parameter adaptive law is designed as

$$\dot{\hat{\Theta}}_{i,1}^{[p]}=\gamma_{i,1}^{[p]}\psi_{i,1}^{[p]}\Psi_{i,1}^2-\tau_{i,1}\hat{\Theta}_{i,1}^{[p]}-\sigma_{i,1}\hat{\Theta}_{i,1}^{[p]1+\varrho},\tag{29}$$

$$\dot{\hat{\rho}}_{i,1}^{[p]}=\Gamma_{i,1}^{[p]}\Psi_{i,1}\tanh\left(\frac{\Psi_{i,1}}{\varsigma_{\rho_i}}\right)-\bar{\tau}_{i,1}\hat{\rho}_{i,1}^{[p]}-\bar{\sigma}_{i,1}\hat{\rho}_{i,1}^{[p]1+\varrho},\tag{30}$$

where $\tau_{i,1}=\bar{\tau}_{i,1}=(\pi/\varrho T_d)^{\frac{2}{2-\varrho}}$, and $\sigma_{i,1}=\dfrac{\pi(2+\varrho)}{2\varrho T_d(1+\varrho)\gamma_{i,1}^{\varrho/2}}$, $\bar{\sigma}_{i,1}=\dfrac{\pi(2+\varrho)}{2\varrho T_d(1+\varrho)\Gamma_{i,1}^{\varrho/2}}$.

Recall the definition of $\zeta_{i,1}(\Psi_{i,1})$ in (20), we have

$$\Psi_{i,1}(z_{i,2}-\zeta_{i,1}(\Psi_{i,1}))\leqslant-|\Psi_{i,1}|(\varpi_{i,1}-|z_{i,2}|_{\max})\leqslant0.\tag{31}$$

According to Lemma 2, substituting (21), (29)–(31) into (28) results in

$$\begin{aligned}\dot{V}_1\leqslant\sum_{i=1}^{M}\Big[&-\frac{\lambda\pi}{\varrho T_d}c_{i,1}\Psi_{i,1}^{2+\varrho}-\frac{\bar{\lambda}\pi}{\varrho T_d}\omega_{i,1}\Psi_{i,1}^{2-\varrho}-\frac{\tau_{i,1}}{\gamma_{i,1}}\tilde{\Theta}_{i,1}^{[p]}\hat{\Theta}_{i,1}^{[p]}\\&-\frac{\sigma_{i,1}}{\gamma_{i,1}}\tilde{\Theta}_{i,1}^{[p]}\hat{\Theta}_{i,1}^{[p]1+\varrho}-\frac{\bar{\tau}_{i,1}}{\Gamma_{i,1}}\tilde{\rho}_{i,1}^{[p]}\hat{\rho}_{i,1}^{[p]}-\frac{\bar{\sigma}_{i,1}}{\Gamma_{i,1}}\tilde{\rho}_{i,1}^{[p]}\hat{\rho}_{i,1}^{[p]1+\varrho}+\vartheta_{i,1}\Big],\end{aligned}\tag{32}$$

where $\vartheta_{i,1}=0.2785\varsigma_{\rho_i}\rho_{i,1}^{[p]*}+\lambda\pi\varsigma_{\Psi_i}/\varrho T_d+\kappa_{i,1}$.

Motivated by the work in [4], in order to reduce the computational complexity inherently embedded in the backstepping procedure, we propose a new predefined-time filter for fractional-order systems. Let α_{i,j_i} pass through the following predefined-time filter with a constant ι_{i,j_i} and a new state variable $\hat{\alpha}_{i,j_i}$. The dynamics of $\hat{\alpha}_{i,j_i}$ can be expressed as

$$\begin{aligned}{}_0^C\mathcal{D}_t^{\alpha}\hat{\alpha}_{i,j_i}=&-\frac{\lambda\pi}{\varrho T_d}\nu_{i,j_i}^{1+\varrho}-\frac{\bar{\lambda}\pi\nu_{i,j_i}^{3-2\varrho}}{\varrho T_d\sqrt{\nu_{i,j_i}^{4-2\varrho}+\varsigma_{\nu_i}^2}}-\iota_{i,j_i}\nu_{i,j_i},\\\hat{\alpha}_{i,j_i}(0)=&\alpha_{i,j_i-1}(0),i=1,2,\cdots,M,j_i=2,\cdots,n_i,\end{aligned}\tag{33}$$

where ι_{i,j_i} and ς_{ν_i} denote positive parameters to be designed. The α-th order derivative of the boundary layer errors $\nu_{i,j_i}=\hat{\alpha}_{i,j_i}-\alpha_{i,j_i}$ is

$${}_0^C\mathcal{D}_t^{\alpha}\nu_{i,j_i}=-\frac{\lambda\pi}{\varrho T_d}\nu_{i,j_i}^{1+\varrho}-\frac{\bar{\lambda}\pi\nu_{i,j_i}^{3-2\varrho}}{\varrho T_d\sqrt{\nu_{i,j_i}^{4-2\varrho}+\varsigma_{\nu_i}^2}}-\iota_{i,j_i}\nu_{i,j_i}+M_{i,j_i}(\cdot),\tag{34}$$

where $M_{i,j_i}(\cdot)$ is a continuous function of the variables $z_{i,1},\cdots,z_{i,j_i},\nu_{i,1},\cdots,\nu_{i,j_i}$, $\Psi_{i,1},\cdots,\Psi_{i,j_i}$, $\hat{\Theta}_{i,1}^{[p]},\cdots,\hat{\Theta}_{i,j_i}^{[p]}$, $\hat{\rho}_{i,1}^{[p]},\cdots,\hat{\rho}_{i,j_i}^{[p]}$ and ${}_0^C\mathcal{D}_t^{\alpha}y_{i,d},{}_0^C\mathcal{D}_t^{\alpha}[{}_0^C\mathcal{D}_t^{\alpha}y_{i,d}]$. Meanwhile, there exists a positive constant B_{i,j_i} such that $M_{i,j_i}(\cdot)\leqslant B_{i,j_i}$ is a given compact set Ξ_{i,j_i}.

Step j_i $(j_i=2,\cdots,n_i-1)$: According to the coordination transformation (19) and (20), one obtains

$$\begin{aligned}\Psi_{i,j_i}=&{}_0^C\mathcal{D}_t^{\alpha}z_{i,j_i}+\mathcal{I}_t^{1-\alpha}\left(\frac{\pi}{\varrho T_d}z_{i,j_i}^{1+\frac{\varrho}{2}}+\frac{\pi}{\varrho T_d}z_{i,j_i}^{1-\frac{\varrho}{2}}\right)\\=&z_{i,j_i+1}+\nu_{i,j_i+1}+\alpha_{i,j_i}+f_{i,j_i}^{[p]}(x)+d_{i,j_i}^{[p]}(t)-{}_0^C\mathcal{D}_t^{\alpha}\bar{\alpha}_{i,j_i}+\mathcal{I}_t^{1-\alpha}\left(\frac{\pi}{\varrho T_d}z_{i,j_i}^{1+\frac{\varrho}{2}}+\frac{\pi}{\varrho T_d}z_{i,j_i}^{1-\frac{\varrho}{2}}\right),\end{aligned}\tag{35}$$

by taking the time derivative of Ψ_{i,j_i}.

To complete the induction, at the j_i-th step, we construct the following Lyapunov function:

$$V_{j_i} = V_{j_i-1} + \sum_{i=1}^{M}\left(\frac{1}{2}\Psi_{i,j_i}^2 + \frac{1}{2}\nu_{i,j_i}^2 + \frac{1}{2\gamma_{i,j_i}}\tilde{\Theta}_{i,j_i}^{[p]2} + \frac{1}{2\Gamma_{i,j_i}}\tilde{\rho}_{i,j_i}^{[p]2}\right), \tag{36}$$

where $\gamma_{i,j_i} > 0$ and $\Gamma_{i,j_i} > 0$ are parameters to be designed. Define $\Theta_{i,j_i}^{[p]*} = \max\{\|\theta_{i,j_i}^{[p]*}\|^2\}$ and $\rho_{i,j_i}^{[p]*} = \delta_{i,j_i}^{[p]} + \bar{d}_{i,j_i}^{[p]}$. Among them, $\tilde{\Theta}_{i,j_i}^{[p]} = \Theta_{i,j_i}^{[p]*} - \hat{\Theta}_{i,j_i}^{[p]}$ and $\tilde{\rho}_{i,j_i}^{[p]} = \rho_{i,j_i}^{[p]*} - \hat{\rho}_{i,j_i}^{[p]}$ represent the parameter estimation errors with $\hat{\rho}_{i,j_i}^{[p]}$ and $\hat{\Theta}_{i,j_i}^{[p]}$ being the estimates of $\Theta_{i,j_i}^{[p]*}$ and $\rho_{i,j_i}^{[p]*}$, respectively.

By (34) and (35), the derivative of V_{i,j_i} is

$$\begin{aligned}\dot{V}_{j_i} =& \dot{V}_{j_i-1} + \sum_{i=1}^{M}\Bigg[\Psi_{i,j_i}(z_{i,j_i+1} + \nu_{i,j_i+1} + \alpha_{i,j_i} + \theta_{i,j_i}^{[p]*T}\varphi_{i,j_i}^{[p]}(x) + \delta_{i,j_i}^{[p]} + d_{i,j_i}^{[p]}(t) \\ & - {}_0^C\mathcal{D}_t^{\alpha}\bar{\alpha}_{i,j_i} + \mathcal{I}_t^{1-\alpha}\left(\frac{\pi}{\varrho T_d}z_{i,j_i}^{1+\frac{\varrho}{2}} + \frac{\pi}{\varrho T_d}z_{i,j_i}^{1-\frac{\varrho}{2}}\right) - \frac{\lambda\pi}{\varrho T_d}\nu_{i,j_i}^{2+\varrho} - \iota_{i,j_i}\nu_{i,j_i}^2 \\ & - \frac{\bar{\lambda}\pi\nu_{i,j_i}^{4-2\varrho}}{\varrho T_d\sqrt{\nu_{i,j_i}^{4-2\varrho} + \varsigma_{\nu_i}^2}} - \nu_{i,j_i}M_{i,j_i}(\cdot) - \frac{1}{\gamma_{i,j_i}}\tilde{\Theta}_{i,j_i}^{[p]}\dot{\hat{\Theta}}_{i,j_i}^{[p]} - \frac{1}{\Gamma_{i,j_i}}\tilde{\rho}_{i,j_i}^{[p]}\dot{\hat{\rho}}_{i,j_i}^{[p]}\Bigg].\end{aligned} \tag{37}$$

Using a similar procedure in Step 1, it can be verified that

$$\Psi_{i,j_i}[\theta_{i,j_i}^{[p]*T}\varphi_{i,j_i}^{[p]}(x) + \varepsilon_{i,j_i}^{[p]} + \bar{d}_{i,j_i}^{[p]}] \leqslant \psi_{i,j_i}^{[p]}\Theta_{i,j_i}^{[p]*}\Psi_{i,j_i}^2\varepsilon_{i,j_i}^{[p]} + \bar{d}_{i,j_i}^{[p]} + \kappa_{i,j_i}, \tag{38}$$

$$-\nu_{i,j_i}M_{i,j_i}(\cdot) \leqslant \frac{1}{2}\nu_{i,j_i}^2 + \frac{1}{2}B_{i,j_i}^2, \tag{39}$$

where $\psi_{i,j_i}^{[p]} = 1/(4\kappa_{i,j_i}\varphi_{i,j_i}^{[p]T}(x_{i,j_i})\varphi_{i,j_i}^{[p]}(x_{i,j_i}))$ and κ_{i,j_i} is a positive constant.

Putting together (37), (38) and (39) yields

$$\begin{aligned}\dot{V}_{j_i} \leqslant& \dot{V}_{j_i-1} + \sum_{i=1}^{M}\Bigg[\Psi_{i,j_i}(z_{i,j_i+1} + \alpha_{i,j_i} - {}_0^C\mathcal{D}_t^{\alpha}\bar{\alpha}_{i,j_i}) - \frac{\lambda\pi}{\varrho T_d}\nu_{i,j_i}^{2+\varrho} - \frac{\bar{\lambda}\pi}{\varrho T_d}\nu_{i,j_i}^{2-\varrho} + \frac{\bar{\lambda}\pi\varsigma_{\nu_i}}{\varrho T_d} + \frac{1}{2}B_{i,j_i}^2 \\ & + \psi_{i,j_i}^{[p]}\Theta_{i,j_i}^{[p]*}\Psi_{i,j_i}^2 + \kappa_{i,j_i} + |\Psi_{i,j_i}|\rho_{i,j_i}^{[p]*} - \frac{1}{\gamma_{i,j_i}}\tilde{\Theta}_{i,j_i}^{[p]}\dot{\hat{\Theta}}_{i,j_i}^{[p]} - \frac{1}{\Gamma_{i,j_i}}\tilde{\rho}_{i,j_i}^{[p]}\dot{\hat{\rho}}_{i,j_i}^{[p]}\Bigg],\end{aligned} \tag{40}$$

Design the parameter adaptation functions as

$$\dot{\hat{\Theta}}_{i,j_i}^{[p]} = \gamma_{i,j_i}\psi_{i,j_i}^{[p]}\Psi_{i,j_i}^2 - \tau_{i,j_i}\hat{\Theta}_{i,j_i}^{[p]} - \sigma_{i,j_i}\hat{\Theta}_{i,j_i}^{[p]1+\varrho}, \tag{41}$$

$$\dot{\hat{\rho}}_{i,j_i}^{[p]} = \Gamma_{i,j_i}\Psi_{i,j_i}\tanh\left(\frac{\Psi_{i,j_i}}{\varsigma_{\rho_i}}\right) - \bar{\tau}_{i,j_i}\hat{\rho}_{i,j_i}^{[p]} - \bar{\sigma}_{i,j_i}\hat{\rho}_{i,j_i}^{[p]1+\varrho}, \tag{42}$$

where $\sigma_{i,j_i} = \dfrac{\pi(2+\varrho)}{2\varrho T_d(1+\varrho)\gamma_{i,j_i}^{\varrho/2}}$, $\bar{\sigma}_{i,j_i} = \dfrac{\pi(2+\varrho)}{2\varrho T_d(1+\varrho)\Gamma_{i,j_i}^{\varrho/2}}$ and $\tau_{i,j_i} = \bar{\tau}_{i,1} = (\pi/\varrho T_d)^{\frac{2}{2-\varrho}}$.

Similar to the previous step, by the definition of $\zeta_{i,j_i}(\Psi_{i,j_i})$, we have

$$\Psi_{i,j_i}(z_{i,j_i+1} - \zeta_{i,j_i}(\Psi_{i,j_i})) \leqslant -|\Psi_{i,j_i}|(\varpi_{i,j_i} - |z_{i,j_i+1}|_{\max}) \leqslant 0. \tag{43}$$

Substituting (21), (41)–(43) into (40) results in

$$\begin{aligned}\dot{V}_{j_i} \leqslant& \sum_{i=1}^{M}\Bigg[-\frac{\lambda\pi}{\varrho T_d}\sum_{k=1}^{j_i}c_{i,k}\Psi_{i,k}^{2+\varrho} - \frac{\bar{\lambda}\pi}{\varrho T_d}\sum_{k=2}^{j_i}\omega_{i,k}\Psi_{i,k}^{2-\varrho} - \frac{\lambda\pi}{\varrho T_d}\sum_{k=1}^{j_i}\nu_{i,j_i}^{2+\varrho} - \frac{\bar{\lambda}\pi}{\varrho T_d}\sum_{k=2}^{j_i}\nu_{i,j_i}^{2-\varrho} \\ & - \sum_{k=1}^{j_i}\frac{\tau_{i,j_i}}{\gamma_{i,j_i}}\tilde{\Theta}_{i,k}^{[p]}\hat{\Theta}_{i,k}^{[p]} - \sum_{k=1}^{j_i}\frac{\sigma_{i,j_i}}{\gamma_{i,j_i}}\tilde{\Theta}_{i,k}^{[p]}\hat{\Theta}_{i,k}^{[p]1+\varrho} - \sum_{k=1}^{j_i}\frac{\bar{\tau}_{i,j_i}}{\Gamma_{i,j_i}}\tilde{\rho}_{i,k}^{[p]}\hat{\rho}_{i,k}^{[p]} - \sum_{k=1}^{j_i}\frac{\bar{\sigma}_{i,j_i}}{\Gamma_{i,j_i}}\tilde{\rho}_{i,k}^{[p]}\hat{\rho}_{i,k}^{[p]1+\varrho} + \vartheta_{i,j_i}\Bigg],\end{aligned} \tag{44}$$

where $\vartheta_{i,j_i} = 0.2785\varsigma_{\rho_i}\rho_{i,j_i}^{[p]*} + (\varsigma_{\Psi_i} + \varsigma_{\nu_i})\lambda\pi/\varrho T_d + \kappa_{i,j_i} + B_{i,j_i}^2/2 + \vartheta_{i,j_i-1}$.

Step n_i***:*** In what follows, the derivative of Ψ_{i,n_i} can be formulated by

$$\dot{\Psi}_{i,n_i} = m_{v_{i,\mu_i}}v_i + h_i(v_i) + f_{i,n_i}^{[p]}(x) + d_{i,n_i}^{[p]}(t) - {}_0^C\mathcal{D}_t^{\alpha}\bar{\alpha}_{i,n_i} + \mathcal{I}_t^{1-\alpha}\left(\frac{\pi}{\varrho T_d}z_{i,n_i}^{1+\frac{\varrho}{2}} + \frac{\pi}{\varrho T_d}z_{i,n_i}^{1-\frac{\varrho}{2}}\right), \tag{45}$$

Consider the Lyapunov function candidate as follows:

$$V = V_{n_i-1} + \sum_{i=1}^{M}\left(\frac{1}{2}\Psi_{i,n_i}^2 + \frac{1}{2}\nu_{i,n_i}^2 + \frac{1}{2\gamma_{i,n_i}}\tilde{\Theta}_{i,n_i}^{[p]2} + \frac{1}{2\Gamma_{i,n_i}}\tilde{\rho}_{i,n_i}^{[p]2}\right), \tag{46}$$

where γ_{i,n_i} and Γ_{i,n_i} are positive constants.

The following inequalities hold:

$$\Psi_{i,n_i}\theta_{i,n_i}^{[p]*T}\varphi_{i,n_i}^{[p]}(x) \leqslant \psi_{i,n_i}^{[p]}\Theta_{i,n_i}^{[p]*}\Psi_{i,n_i}^2 + \kappa_{i,n_i}, \tag{47}$$

$$\Psi_{i,n_i}(\varepsilon_{i,n_i}^{[p]} + \bar{d}_{i,n_i}^{[p]}) \leqslant |\Psi_{i,n_i}|\rho_{i,n_i}^{[p]*}, \tag{48}$$

$$\Psi_{i,n_i}h_i(v_i) \leqslant \frac{1}{2}\Psi_{i,n_i}^2 + \frac{1}{2}H_i^2, \tag{49}$$

$$-\nu_{i,n_i}M_{i,n_i}(\cdot) \leqslant \frac{1}{2}\nu_{i,n_i}^2 + \frac{1}{2}B_{i,n_i}^2, \tag{50}$$

where $\psi_{i,n_i}^{[p]} = 1/(4\kappa_{i,n_i}\varphi_{i,n_i}^{[p]T}(x_{i,n_i})\varphi_{i,n_i}^{[p]}(x_{i,n_i}))$ and κ_{i,n_i} is a positive parameter.

By differentiating the Lyapunov function V and using (47)–(50), it can be obtained that

$$\begin{aligned}\dot{V} \leqslant \dot{V}_{n_i-1} + \sum_{i=1}^{M}\Bigg[&\Psi_{i,n_i}(m_{v_{i,\mu_i}}v_i - {}_0^C\mathcal{D}_t^{\alpha}\bar{\alpha}_{i,n_i}) + \frac{\Psi_{i,n_i}^2}{2} - \frac{\lambda\pi}{\varrho T_d}\nu_{i,n_i}^{2+\varrho} - \frac{\bar{\lambda}\pi}{\varrho T_d}\nu_{i,n_i}^{2-\varrho} + \varsigma_{\nu_i} + \psi_{i,n_i}^{[p]}\Theta_{i,n_i}^{[p]*}\Psi_{i,n_i}^2 \\ &+ \frac{1}{2}H_i^2 + \kappa_{i,n_i} + |\Psi_{i,n_i}|\rho_{i,n_i}^{[p]*} - \frac{1}{\gamma_{i,n_i}}\tilde{\Theta}_{i,n_i}^{[p]}\dot{\hat{\Theta}}_{i,n_i}^{[p]} - \frac{1}{\Gamma_{i,n_i}}\tilde{\rho}_{i,n_i}^{[p]}\dot{\hat{\rho}}_{i,n_i}^{[p]} + \frac{1}{2}B_{i,n_i}^2\Bigg],\end{aligned} \tag{51}$$

where $\psi_{i,n_i}^{[p]} = 1/(4\kappa_{i,n_i}\varphi_{i,n_i}^{[p]T}(x_{i,n_i})\varphi_{i,n_i}^{[p]}(x_{i,n_i}))$ and κ_{i,n_i} is a positive constant.

According to (51), the adaptive updated laws are designed as follows:

$$\dot{\hat{\Theta}}_{i,n_i}^{[p]} = \gamma_{i,n_i}\psi_{i,n_i}^{[p]}\Psi_{i,n_i}^2 - \tau_{i,n_i}\hat{\Theta}_{i,n_i}^{[p]} - \sigma_{i,n_i}\hat{\Theta}_{i,n_i}^{[p]1+\varrho}, \tag{52}$$

$$\dot{\hat{\rho}}_{i,n_i}^{[p]} = \Gamma_{i,n_i}\Psi_{i,n_i}\tanh\left(\frac{\Psi_{i,n_i}}{\varsigma_{\rho_i}}\right) - \bar{\tau}_{i,n_i}\hat{\rho}_{i,n_i}^{[p]} - \bar{\sigma}_{i,n_i}\hat{\rho}_{i,n_i}^{[p]1+\varrho}, \tag{53}$$

where $\sigma_{i,n_i} = \dfrac{\pi(2+\varrho)}{2\varrho T_d(1+\varrho)\gamma_{i,n_i}^{\varrho/2}}$, $\bar{\sigma}_{i,n_i} = \dfrac{\pi(2+\varrho)}{2\varrho T_d(1+\varrho)\Gamma_{i,n_i}^{\varrho/2}}$ and $\tau_{i,n_i} = \bar{\tau}_{i,1} = (\pi/\varrho T_d)^{\frac{2}{2-\varrho}}$.

From the definition of $m_{v_{i,\mu_i}}$, substituting (22), (52)–(53) into (51), one has

$$\begin{aligned}\dot{V} \leqslant \sum_{i=1}^{M}\Bigg[&-\frac{\lambda\pi}{\varrho T_d}\sum_{k=1}^{n_i}c_{i,k}\Psi_{i,k}^{2+\varrho} - \frac{\bar{\lambda}\pi}{\varrho T_d}\sum_{k=1}^{n_i}\omega_{i,k}\Psi_{i,k}^{2-\varrho} - \frac{\lambda\pi}{\varrho T_d}\sum_{k=2}^{n_i}\nu_{i,k}^{2+\varrho} - \frac{\bar{\lambda}\pi}{\varrho T_d}\sum_{k=2}^{n_i}\nu_{i,k}^{2-\varrho} \\ &- \sum_{k=1}^{n_i}\frac{\tau_{i,k}}{\gamma_{i,k}}\tilde{\Theta}_{i,k}^{[p]}\hat{\Theta}_{i,k}^{[p]} - \sum_{k=1}^{n_i}\frac{\sigma_{i,k}}{\gamma_{i,k}}\tilde{\Theta}_{i,k}^{[p]}\hat{\Theta}_{i,k}^{[p]1+\varrho} - \sum_{k=1}^{n_i}\frac{\bar{\tau}_{i,k}}{\Gamma_{i,k}}\tilde{\rho}_{i,k}^{[p]}\hat{\rho}_{i,k}^{[p]} - \sum_{k=1}^{n_i}\frac{\bar{\sigma}_{i,k}}{\Gamma_{i,k}}\tilde{\rho}_{i,k}^{[p]}\hat{\rho}_{i,k}^{[p]1+\varrho} + \vartheta_{i,n_i}\Bigg],\end{aligned} \tag{54}$$

where $\vartheta_{i,n_i} = 0.2785\varsigma_{\rho_i}\rho_{i,n_i}^{[p]*} + (\varsigma_{\Psi_i} + \varsigma_{\nu_i})\lambda\pi/\varrho T_d + \kappa_{i,n_i} + H_i^2/2 + B_{i,n_i}^2/2 + \vartheta_{i,n_i-1}$.

3.2. Stability Analysis

In this subsection, the stability of the considered system is readily verified. The major result of the proposed design is stated in the following theorem.

Theorem 2. *Consider switched fractional-order system (14) with input saturation (15) under Assumption 1. Given predefined-time filter (33), actual controller (22), intermediate control functions (21), and parameter adaptation functions (29), (30), (41), (42) and (52) and (53), then all the closed-loop signals remain bounded and closed-loop system (14) is practically predefined-time stable. Furthermore, the tracking error can tend to a small region of the origin within a predefined time, and the impact of the input saturation is compensated simultaneously.*

Proof 2. *Applying Young's inequality to (54) yields* $\tilde{\Theta}_{i,j_i}^{[p]}\hat{\Theta}_{i,j_i}^{[p]} \leqslant -\tilde{\Theta}_{i,j_i}^{[p]2}/2 + \Theta_{i,j_i}^{[p]*2}/2$, *and* $\tilde{\rho}_{i,j_i}^{[p]}\hat{\rho}_{i,j_i}^{[p]} \leqslant -\tilde{\rho}_{i,j_i}^{[p]2}/2 + \rho_{i,j_i}^{[p]*2}/2$. *Substituting the above two inequalities into (54), one has*

$$\begin{aligned}\dot{V} \leqslant \sum_{i=1}^{M}\Bigg[&-\frac{\lambda\pi}{\varrho T_d}\sum_{k=1}^{n_i}c_{i,k}\Psi_{i,k}^{2+\varrho} - \frac{\bar{\lambda}\pi}{\varrho T_d}\sum_{k=1}^{n_i}\omega_{i,k}\Psi_{i,k}^{2-\varrho} - \frac{\lambda\pi}{\varrho T_d}\sum_{k=2}^{n_i}\nu_{i,k}^{2+\varrho} - \frac{\bar{\lambda}\pi}{\varrho T_d}\sum_{k=2}^{n_i}\nu_{i,k}^{2-\varrho} \\ &- \sum_{k=1}^{n_i}\frac{\tau_{i,k}}{2\gamma_{i,k}}\tilde{\Theta}_{i,k}^{[p]2} - \sum_{k=1}^{n_i}\frac{\sigma_{i,k}}{\gamma_{i,k}}\tilde{\Theta}_{i,k}^{[p]}\hat{\Theta}_{i,k}^{[p]1+\varrho} - \sum_{k=1}^{n_i}\frac{\bar{\tau}_{i,k}}{2\Gamma_{i,k}}\tilde{\rho}_{i,k}^{[p]2} - \sum_{k=1}^{n_i}\frac{\bar{\sigma}_{i,k}}{\Gamma_{i,k}}\tilde{\rho}_{i,k}^{[p]}\hat{\rho}_{i,k}^{[p]1+\varrho} + \vartheta_{i,n_i}\Bigg],\end{aligned} \tag{55}$$

where $\vartheta_i = \vartheta_{i,n_i} + \frac{\tau_{i,n_i}}{2\gamma_{i,n_i}} \sum_{k=1}^{n_i} \Theta_{i,k}^{[p]*2} + \frac{\bar{\tau}_{i,n_i}}{2\Gamma_{i,n_i}} \sum_{k=1}^{n_i} \rho_{i,k}^{[p]*2}$.

Furthermore, applying Lemma 3 to the above inequality, we have

$$\left(\frac{\tilde{\Theta}_{i,j_i}^{[p]}}{2\gamma_{i,j_i}^{[p]}} \right)^{1-\frac{\varrho}{2}} \leqslant \frac{\tilde{\Theta}_{i,j_i}^{[p]2}}{2\gamma_{i,j_i}^{[p]}} + \iota_{\tilde{\Theta}_i}, \tag{56}$$

$$\left(\frac{\tilde{\rho}_{i,j_i}^{[p]}}{2\Gamma_{i,j_i}^{[p]}} \right)^{1-\frac{\varrho}{2}} \leqslant \frac{\tilde{\rho}_{i,j_i}^{[p]2}}{2\Gamma_{i,j_i}^{[p]}} + \iota_{\tilde{\rho}_i}, \tag{57}$$

where $\iota_{\tilde{\Theta}_i} = \frac{\varrho}{2} \left(\frac{2-\varrho}{2} \right)^{\frac{2-\varrho}{\varrho}}$ *and* $\iota_{\tilde{\rho}_i} = \frac{\varrho}{2} \left(\frac{2-\varrho}{2} \right)^{\frac{2-\varrho}{\varrho}}$.

Consequently, with the help of Lemma 4, we have

$$\tilde{\Theta}_{i,j_i}^{[p]} \hat{\Theta}_{i,j_i}^{[p]1+\varrho} \leqslant \frac{1+\varrho}{2+\varrho} (\Theta_{i,j_i}^{[p]*2+\varrho} - \tilde{\Theta}_{i,j_i}^{[p]2+\varrho}), \tag{58}$$

$$\tilde{\rho}_{i,j_i}^{[p]} \hat{\rho}_{i,j_i}^{[p]1+\varrho} \leqslant \frac{1+\varrho}{2+\varrho} (\rho_{i,j_i}^{[p]*2+\varrho} - \tilde{\rho}_{i,j_i}^{[p]2+\varrho}). \tag{59}$$

By further substituting (56)-(59) into (55), it can be deduced that

$$\begin{aligned} \dot{V} \leqslant \sum_{i=1}^{M} \Bigg[& - \frac{c_{i,j_i} 2^{1+\frac{\varrho}{2}} \lambda\pi}{\varrho T_d n_i^{\frac{\varrho}{2}}} \left(\sum_{k=1}^{n_i} \frac{1}{2} \Psi_{i,k}^2 \right)^{1+\frac{\varrho}{2}} - \frac{2^{1+\frac{\varrho}{2}} \lambda\pi}{\varrho T_d n_i^{\frac{\varrho}{2}}} \left(\sum_{k=2}^{n_i} \frac{1}{2} \nu_{i,k}^2 \right)^{1+\frac{\varrho}{2}} - \frac{\sigma_{i,k}\pi}{\varrho T_d n_i^{\frac{\varrho}{2}}} \left(\sum_{k=1}^{n_i} \frac{\tilde{\Theta}_{i,k}^{[p]}}{2\gamma_{i,k}} \right)^{1+\frac{\varrho}{2}} \\ & - \frac{\bar{\sigma}_{i,k}\pi}{\varrho T_d n_i^{\frac{\varrho}{2}}} \left(\sum_{k=1}^{n_i} \frac{\tilde{\rho}_{i,k}^{[p]}}{2\Gamma_{i,k}} \right)^{1+\frac{\varrho}{2}} - \frac{\omega_{i,j_i}\bar{\lambda}\pi}{\varrho T_d 2^{-1+\frac{\varrho}{2}}} \left(\sum_{k=1}^{n_i} \frac{1}{2} \Psi_{i,k}^2 \right)^{1-\frac{\varrho}{2}} - \frac{2^{1-\frac{\varrho}{2}}\bar{\lambda}\pi}{\varrho T_d} \left(\sum_{k=2}^{n_i} \frac{1}{2} \nu_{i,k}^2 \right)^{1-\frac{\varrho}{2}} \\ & - \frac{\tau_{i,k}\pi}{\varrho T_d} \left(\sum_{k=1}^{n_i} \frac{\tilde{\Theta}_{i,k}^{[p]}}{2\gamma_{i,k}} \right)^{1-\frac{\varrho}{2}} - \frac{\bar{\tau}_{i,k}\pi}{\varrho T_d} \left(\sum_{k=1}^{n_i} \frac{\tilde{\rho}_{i,k}^{[p]}}{2\Gamma_{i,k}} \right)^{1-\frac{\varrho}{2}} \Bigg] + \vartheta \end{aligned} \tag{60}$$

where $\vartheta = \sum_{i=1}^{M} \left(\vartheta_i + \sum_{k=1}^{n_i} \left(\iota_{\tilde{\Theta}_i} + \iota_{\tilde{\rho}_i} + \frac{1+\varrho}{2+\varrho} \Theta_{i,j_i}^{[p]*2+\varrho} + \frac{1+\varrho}{2+\varrho} \rho_{i,j_i}^{[p]*2+\varrho} + \sum_{k=1}^{n_i} \frac{\tau_{i,k}}{2\gamma_{i,k}^{[p]}} \Theta_{i,k}^{[p]*2} + \sum_{k=1}^{n_i} \frac{\bar{\tau}_{i,k}}{2\Gamma_{i,k}^{[p]}} \rho_{i,k}^{[p]*2} \right) \right)$.

Let $a = \min\{c_{i,1}, c_{i,2}, \cdots, c_{i,j_i}, 1\}$ *and* $b = \min\{\omega_{i,1}, \omega_{i,2}, \cdots, \omega_{i,j_i}, 1\}$. *Then, according to Lemma 5, one can easily obtain*

$$\begin{aligned} \dot{V} \leqslant & - \frac{a\pi}{\varrho T_d} \sum_{i=1}^{M} \left[\sum_{k=1}^{n_i} \left(\frac{1}{2} \Psi_{i,k}^2 + \frac{1}{2} \nu_{i,k}^2 + \frac{1}{2\gamma_{i,k}} \tilde{\Theta}_{i,k}^{[p]} + \frac{1}{2\Gamma_{i,k}} \tilde{\rho}_{i,k}^{[p]} \right) \right]^{1+\frac{\varrho}{2}} \\ & - \frac{b\pi}{\varrho T_d} \sum_{i=1}^{M} \left[\sum_{k=1}^{n_i} \left(\frac{1}{2} \Psi_{i,k}^2 + \frac{1}{2} \nu_{i,k}^2 + \frac{1}{2\gamma_{i,k}} \tilde{\Theta}_{i,k}^{[p]} + \frac{1}{2\Gamma_{i,k}} \tilde{\rho}_{i,k}^{[p]} \right) \right]^{1-\frac{\varrho}{2}} + \vartheta \\ = & - \frac{\pi}{\varrho T_d} (aV^{1+\frac{\varrho}{2}} + bV^{1-\frac{\varrho}{2}}) + \vartheta. \end{aligned} \tag{61}$$

According to Theorem 1, it is known that for any $t \geqslant T_d$, *the solution of system (14) will converge to the following compact set:*

$$\Omega = \left\{ \lim_{t \to T_p} V | V \leqslant \min \left\{ \left(\frac{2\vartheta\varrho T_d}{\pi b} \right)^{\frac{2}{2-\varrho}}, \left(\frac{2\vartheta\varrho T_d}{\pi a} \right)^{\frac{2}{2+\varrho}} \right\} \right\},$$

where the settling-time is given by $T_p \leqslant T_{\max} = \sqrt{2} T_d / \sqrt{ab}$.

According to the definition of V, *it is concluded from (61) that the auxiliary function* Ψ_{i,j_i}, *adaptive parameter errors* $\tilde{\Theta}_{i,j_i}^{[p]}$ *and* $\tilde{\rho}_{i,j_i}^{[p]}$ *(*$i = 1, 2, \cdots, M$, $j_i = 1, 2, \cdots, n_i$*), and filtering errors* ν_{i,j_i} *(*$j_i = 2, \cdots, n_i$*) reach the boundary of* Ω *after a predefined time. Taking into account* $\tilde{\Theta}_{i,j_i}^{[p]} = \Theta_{i,j_i}^{[p]*} - \hat{\Theta}_{i,j_i}^{[p]}$ *and* $\tilde{\rho}_{i,j_i}^{[p]} = \rho_{i,j_i}^{[p]*} - \hat{\rho}_{i,j_i}^{[p]}$, *the boundedness of* $\hat{\Theta}_{i,j_i}^{[p]}$ *and* $\hat{\rho}_{i,j_i}^{[p]}$ *can be guaranteed. Then, the virtual control functions* α_{i,j_i} *and* ν_i *also remain bounded. Furthermore, from the definitions of the auxiliary function and the coordinate transformation, it can be concluded that all closed-loop signals of system (14) remain bounded. In other words, when the error variables are located at the auxiliary function, we have* $\Psi_{i,j_i} = 0$ *for* $t \geqslant T_p$. *When* $\Psi_{i,j_i} = 0$, *the following equation holds:*

$$\mathcal{I}_t^{1-\alpha} z_{i,j_i} + \mathcal{I}_t^{2-\alpha} \left(\frac{\pi}{\varrho T_d} z_{i,j_i}^{1+\frac{\varrho}{2}} + \frac{\pi}{\varrho T_d} z_{i,j_i}^{1-\frac{\varrho}{2}} \right) = 0. \tag{62}$$

Taking the ${}_0\mathcal{D}_t^{2-\alpha}$ *derivative and using the properties of the RL derivative, the following equation holds:*

$$\dot{z}_{i,j_i} = -\frac{\pi}{\varrho T_d} z_{i,j_i}^{1+\frac{\varrho}{2}} - \frac{\pi}{\varrho T_d} z_{i,j_i}^{1-\frac{\varrho}{2}}. \tag{63}$$

Based on Lemma 7, we can prove that $z_{i,1}$ *is predefined-time convergent. When the auxiliary function satisfies* $\Psi_{i,1} = 0$, $z_{i,1}$ *will converge to zero after a predefined-time which is bounded by* $T_p' \leqslant T_{\max}' = T_d$. *From the initial time* $t = 0$, *the tracking error* $z_{i,1}(t)$ *is achieved by the predefined-time, and the settling-time upper boundary is predetermined as* $T_{z_{i,1}} = T_p + T_p'$ *by designers. The proof is completed.*

Remark 3. *In fact, compared with the first-order linear filter commonly used in the dynamic surface control techniques for integer-order systems, the proposed predefined-time filter is designed for fractional-order systems and is able to directly set the convergence time of the filtering error. Such a filter also eliminates the complexity explosion problem caused by repeatedly deriving the intermediate control law during the backstepping recursive design procedure. Owing to the existence of the term* $\nu_{i,j_i}^{1-\varrho}$, *the derivative of the filtering error tends to infinity when* $\nu_{i,j_i}^{1-\varrho}$ *tends to zero, and the singularity problem is avoided by using the function* $1/\sqrt{(\cdot)^2+\varsigma^2}$ *in this paper.*

Remark 4. ${}_0^{RL}\mathcal{D}_t^{\alpha}(\cdot)$ *is the* α*-order RL derivative. From Definition 1-2 and Property 1, it is known that* $d(\mathcal{I}_t^{1-\alpha}(\cdot))/(dt)$ *in (23) coincides with the* α*-th order RL derivative other than the* α*-th order Caputo derivative, i.e.* $d(\mathcal{I}_t^{1-\alpha}(\cdot))/(dt) = {}_0^{RL}\mathcal{D}_t^{\alpha}(\cdot)$. *According to the relationship between the Caputo and RL derivatives, if* $0 < \alpha < 1$, *we have* ${}_0^{C}\mathcal{D}_t^{\alpha} z_{i,1} = {}_0^{RL}\mathcal{D}_t^{\alpha} z_{i,1} - z_{i,1}(0)/(\Gamma(1-\alpha)t^{\alpha})$. *It is clear from the above description that, if* $z_{i,1}(0) > 0$, *one can immediately have* ${}_0^{C}\mathcal{D}_t^{\alpha} z_{i,1}(0) \leqslant {}_0^{RL}\mathcal{D}_t^{\alpha} z_{i,1}(0)$. *Indeed, the term* $t^{-\alpha}$ *will monotonically decrease towards* 0 *as time goes to infinity.*

Remark 5. *In Eqs. (20), (31) and (43), we suppose that the coefficient* ϖ_{i,j_i} *is greater than the maximum of the absolute error* $|z_{i,j_i+1}|$, *which implies that the error* $|z_{i,j_i}|$, $j_i = 1, 2, \cdots, n_i - 1$, *is a priori bounded. This fact is usually possible since the solution of a fractional-order system is restricted to a bounded domain. Meanwhile, the effective determination of the parameter* ϖ_{i,j_i} *deserves attention in practice, and relative results can be found in many available applications. For example, the trial-and-error method can be successfully used to determine the actual value of the parameter* ϖ_{i,j_i} *[32].*

Remark 6. *So far, most of the results on predefined time control have designed their controllers based on the sign function [39−41, 43]. Although the fast convergence behavior is achieved, the chattering phenomenon still exists. Therefore, similar to [4], we introduce a function* $(\cdot)^2/\sqrt{(\cdot)^2+\varsigma^2}$ *to avoid the possible chattering phenomenon. Note that* ς *cannot be too small; otherwise, the existence of the term* $(\cdot)^2/\sqrt{(\cdot)^2+\varsigma^2}$ *will lead to the occurrence of the chattering phenomenon.*

Remark 7. *For switched nonlinear systems, the proposed method uses the common Lyapunov function approach (see [17,21, 23−25]) to construct the adaptive switching control law instead of using the multiple Lyapunov function approach and the average dwell time theory [18, 22]. As a result, the switching signal is no longer required to satisfy the predefined dwell time.*

Remark 8. *In fact, the radius of the tracking error region is determined by the control parameters. To guarantee a small tracking error, it is necessary to increase the values of parameters* c_{i,j_i}, γ_{i,j_i} *and* Γ_{i,j_i}, *or decrease the values of parameters* σ_{i,j_i}, τ_{i,j_i}, $\bar{\sigma}_{i,j_i}$, $\bar{\tau}_{i,j_i}$, ϱ *and* T_d. *Note that if the controller's predetermined time* T_d *or the saturation value of the selected actuator is not reasonable, then the required stable time exceeds the actuator's capability.*

4. Simulations

This section illustrates the applicability and effectiveness of the proposed control strategy by two simulation examples.

Example 1: Consider the following MIMO switched nonstrict feedback nonlinear system [23]:

$$\begin{cases} {}_0^{C}\mathcal{D}_t^{\alpha} x_{11} = x_{12} + f_{11}^{[\sigma(t)]}(x) + d_{11}^{[\sigma(t)]}(t), \\ {}_0^{C}\mathcal{D}_t^{\alpha} x_{12} = f_{12}^{[\sigma(t)]}(x) + d_{12}^{[\sigma(t)]}(t) + u_1, \\ y_1 = x_{11}, \\ {}_0^{C}\mathcal{D}_t^{\alpha} x_{21} = x_{22} + f_{21}^{[\sigma(t)]}(x) + d_{21}^{[\sigma(t)]}(t), \\ {}_0^{C}\mathcal{D}_t^{\alpha} x_{22} = f_{22}^{[\sigma(t)]}(x) + d_{22}^{[\sigma(t)]}(t) + u_2, \\ y_2 = x_{21}, \end{cases} \tag{64}$$

where $\sigma(t) \in \{1, 2\}$ denotes the switching signal. $f_{11}^{[1]} = x_{12}\sin(x_{11}x_{12})$, $f_{12}^{[1]} = \sin(x_{11}x_{12}^2) + \exp(x_{11}x_{12})$, $f_{21}^{[1]} = x_{22}\exp(0.5x_{21}x_{22})$ and $f_{22}^{[1]} = 3\cos(x_{21}x_{22}) + x_{21}x_{22}^2$. $f_{11}^{[2]} = 0$, $f_{12}^{[2]} = \sin(x_{11}x_{12}) + x_{11}^2 x_{12}$ $f_{21}^{[2]} = 0$ and $f_{22}^{[2]} = \sin(x_{21}x_{22}^2) + x_{21}x_{22}$. We chose the external disturbances as $d_{11}^{[1]}(t) = d_{12}^{[1]}(t) = 0.2\sin(t) + 0.4\cos(t)$, $d_{21}^{[1]}(t) = d_{22}^{[1]}(t) = 0.3\sin(t) + 0.2\cos(t)$, $d_{11}^{[2]}(t) = d_{12}^{[2]}(t) = 0.2\sin(t)$ and $d_{21}^{[2]}(t) = d_{22}^{[2]}(t) = 0.3\sin(t)$. The switching signal is selected as $\sigma(t) = 2$

in $[5s, 9s] \cup [14s, 18s]$; $\sigma(t) = 1$, otherwise.

The design parameters of this example are chosen as $T_d = 1s$, $\varrho = 69/101$, $c_{11} = 0.5$, $c_{12} = 5$, $c_{21} = 0.5$, $c_{22} = 5$, $\omega_{11} = 0.35$, $\omega_{12} = 8$, $\omega_{21} = 0.3$, $\omega_{22} = 7$, $\kappa_{11} = \kappa_{12} = \kappa_{21} = \kappa_{22} = 2$, $\iota_{12} = \iota_{22} = 10$ and $\Gamma_{i,j_i} = \gamma_{i,j_i} = 100$. The choice of parameters ϖ_{i,j_i} depends on the maximum values of the errors. In anticipation, we set $\varpi_{i,j_i} = 10$. The nonlinear functions $\zeta_{i,j_i}(\Psi_{i,j_i})$ are chosen as $\zeta_{i,j_i}(\Psi_{i,j_i}) = 2\tanh(\Psi_{i,j_i})$. The conditions $\Psi_{i,j_i}\zeta_{i,j_i}(\Psi_{i,j_i}) > \varpi_{i,j_i}|\Psi_{i,j_i}| > 0$ are well satisfied. In this example, the Gaussian membership functions are defined as $\mu_{F^l_{i,j_i}}(x_{i,j_i}) = \exp(-(x_{i,j_i}+3-l)^2/4)$ with $l = 1,2,3,4,5$, $i = 1,2$ and $j_i = 1,2$ which are uniformly distributed on $[-5,5]$. The initial condition is chosen as $[x_{11}(0), x_{12}(0), x_{21}(0), x_{22}(0)]^T = [0.3, 0.5, 0.3, 0.5]^T$, $[\hat{\Theta}_{11}(0), \hat{\Theta}_{12}(0), \hat{\Theta}_{21}(0), \hat{\Theta}_{22}(0)]^T = [0.4, 0.4, 0.4, 0.4]^T$ and $[\hat{\rho}_{11}(0), \hat{\rho}_{12}(0), \hat{\rho}_{21}(0), \hat{\rho}_{22}(0)]^T = [0.6, 0.6, 0.6, 0.5]^T$. The input saturation limits are set as $\bar{u}_i = 7$ and $\underline{u}_i = -7$.

The simulation results are shown in Figures 1–6. Figure 1 depicts the tracking performance of the presented control strategy. It is observed that the trajectories of the reference signals $y_{i,d}$ (i = 1, 2) can be tracked rapidly and precisely, illustrating the rationality of the designed filter. Figure 2 shows the trajectories of state variables $x_{i,2}$. The adaptive parameters Θ_{i,j_i} and ρ_{i,j_i} (i = 1, 2; j_i=1,2) are presented in Figure 3. Figure 4 displays the curves of controllers $u_i(v_i)$ and v_i, which are constrained by input saturation with $\bar{u}_i = 7$ and $\underline{u}_i = -7$. As depicted in these figures, it is obvious that the practical settling time is less than the predefined time $T_p = \sqrt{2}T_d/\sqrt{ab} \approx 3.38s$. The practical convergence time of the tracking error is much less than $T_{z_{i1}} = T_p + T'_p = 4.38s$. Moreover, for the case that the switching signal occurs before the practical settling time, it follows from Figures 5 and 6 that, the tracking errors and filtering errors at different settling times $T_d = 1s$, $T_d = 2s$ and $T_d = 5s$ can all be retained to zeros within a small region, but variations exist in the convergence rate. According to Figure 6, we can see that the new filtering algorithm proposed in this paper can directly set the convergence time of the filtering error. Hence, it can be concluded that the proposed control method achieves the control objective successfully.

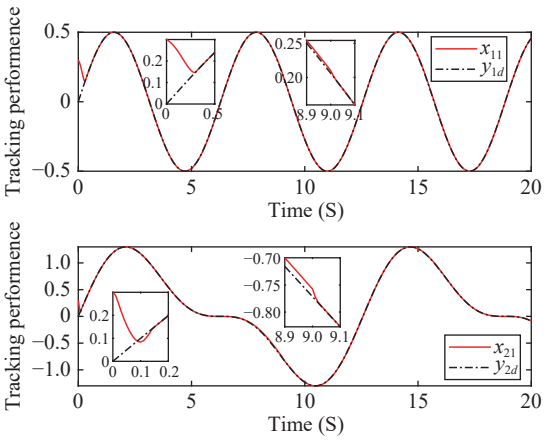

Figure 1. Example 1: Trajectories of system output y_i and the reference signal y_{id} (i=1, 2).

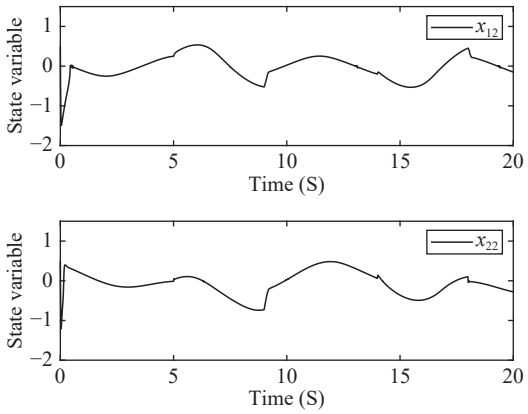

Figure 2. Example 1: Trajectories of state variables x_{12} and x_{22}.

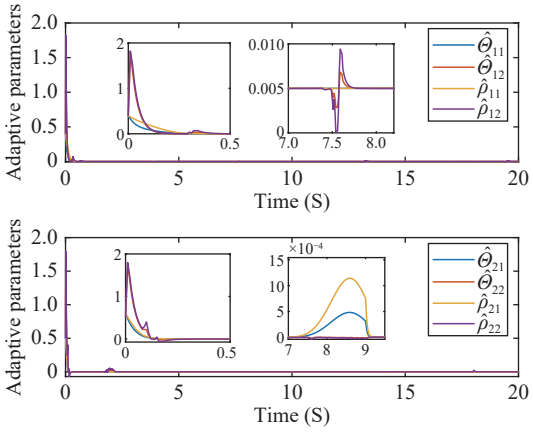

Figure 3. Example 1: Trajectories of the adaptive parameters $\hat{\Theta}_{i,j_i}$ and $\hat{\rho}_{i,j_i}$ (i=1, 2; j_i=1, 2).

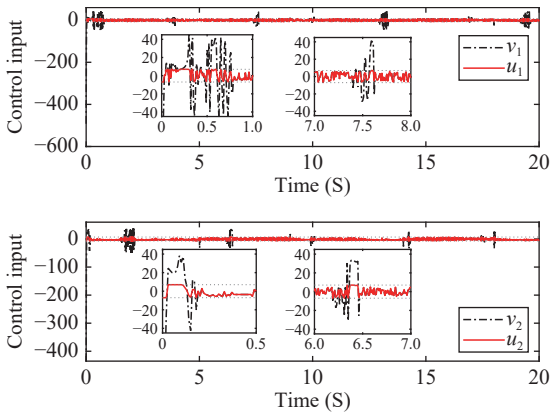

Figure 4. Example 1: Trajectories of the saturation input u_i and v_i.

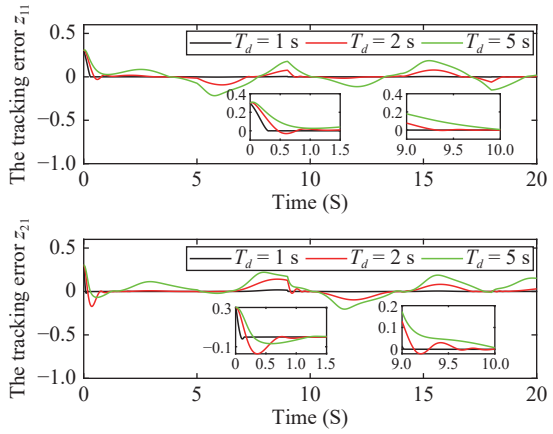

Figure 5. Example 1: Trajectories of the tracking errors z_{11} and z_{21} based on the different settling time.

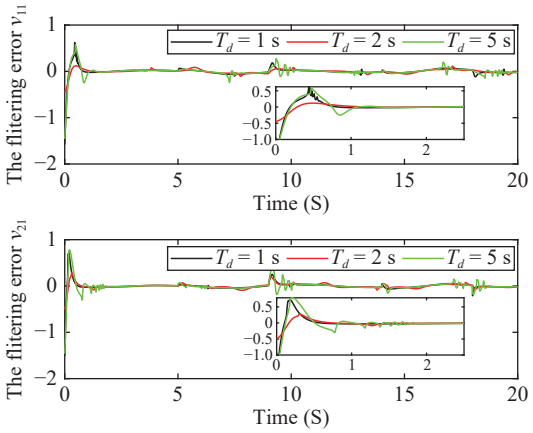

Figure 6. Example 1: Trajectories of the filtering errors v_{11} and v_{21} based on the different settling time.

Remark 9. *It is seen in Figures 1 and 4 that, achieving fast convergence at the same time implies that the control input needs to be large enough. Therefore, the trade-off between better tracking performance and less control energy is a constant consideration for researchers, where the consideration of the input saturation in system (14) can be treated as a reasonable solution. However, as shown from Figures 4 and 9, the obvious deficiency is that, the control input results are not smooth enough due to switching. Theoretically, the term* $(\cdot)^2/\sqrt{(\cdot)^2+\varsigma^2}$ *is similar to the sign function if* ς *is too small, which obviously results in the chattering phenomenon.*

Example 2: To further demonstrate the feasibility and effectiveness of the proposed scheme in this article, we consider a practically predefined-time control problem [49] of a permanent magnet synchronous motor model with a smooth air gap.

$$\begin{cases} {}_0^C\mathcal{D}_t^{\alpha}\omega = -k(i_q-\omega), \\ {}_0^C\mathcal{D}_t^{\alpha}i_q = -i_q-\omega i_d+\upsilon\omega+g_1u_q, \\ {}_0^C\mathcal{D}_t^{\alpha}i_d = -i_d+\omega i_q+g_2u_d, \end{cases} \tag{65}$$

where ω, i_q and i_d stand for the rotor angular velocity, the current of the d axis and the current of the q axis, respectively. u_d and u_q denote the $d-q$ axis voltage. Assume that only two controllers u_1 and u_2 are applied to system (65). The system parameters are set as $k=4$, $\upsilon=1$, $g_1=20$ and $g_2=15$. In this simulation, we denote $x_{11}=\omega$, $x_{12}=i_q$ and $x_{21}=i_d$. Then, the fractional-order dynamic equation of this mechanical system can be transformed to a typical form (64) where $f_{11}^{[1]}=-kx_{11}$, $g_{11}^{[1]}=k$, $f_{12}^{[1]}=\upsilon x_{11}-x_{12}-x_{11}x_{21}$, $g_{12}^{[1]}=g_1$, $f_{21}^{[1]}=-x_{21}-x_{11}x_{12}$, $g_{21}^{[1]}=g_2$, $f_{11}^{[2]}=x_{12}+x_{11}\sin(x_{12})$, $g_{11}^{[2]}=1$, $f_{12}^{[2]}=2x_{11}^2/3+x_{12}^2\cos(x_{12})/3+x_{11}^2\sin(x_{11}x_{12})/3$, $g_{12}^{[2]}=1$, $f_{21}^{[2]}=-\sin(x_{21})-x_{11}x_{12}$, and $g_{21}^{[2]}=1$.

The fractional order is selected as $\alpha=0.98$ and the reference signals are assumed to be $y_{1,d}=0.5\sin t$ and $y_{1,d}=\sin(0.5t)+0.5\sin t$. The design parameters of this example are chosen as $T_d=1s$, $\varrho=69/101$, $c_{11}=0.35$, $c_{12}=8$, $c_{21}=0.3$, $\omega_{11}=0.5$, $\omega_{12}=5$ and $\omega_{21}=0.5$. Other parameters are selected the same with Example 1.

Figures 7−11 depict the corresponding simulation results. The qualitative analysis results of this example are identical to that of Example 1. From these figures, we can observe that the tracking error of the presented method can be tuned to a smaller neighborhood of the origin. Moreover, the given upper boundary on the settling-time provides the user with more practical metrics to understand and tune the system performance.

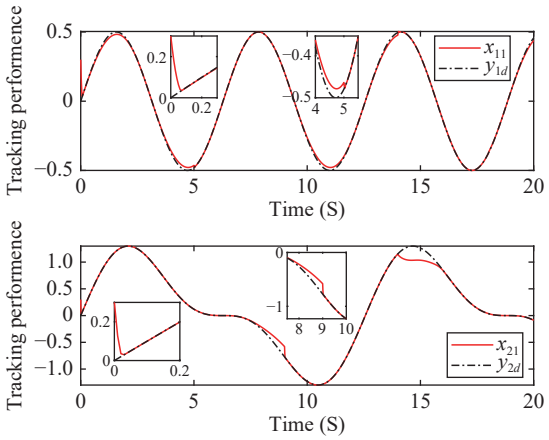

Figure 7. Example 2: Trajectories of system output y_i and the reference signal y_{id}, $i = 1, 2$.

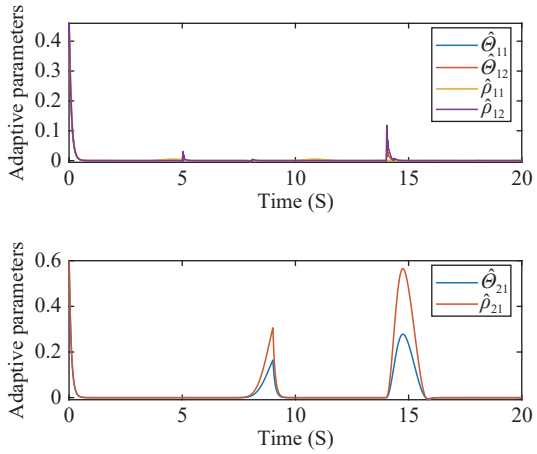

Figure 8. Example 2: Trajectories of the adaptive parameters $\hat{\Theta}_{i,j_i}$ and $\hat{\rho}_{1,j_i}$ (i=1, 2; j_i=1, 2).

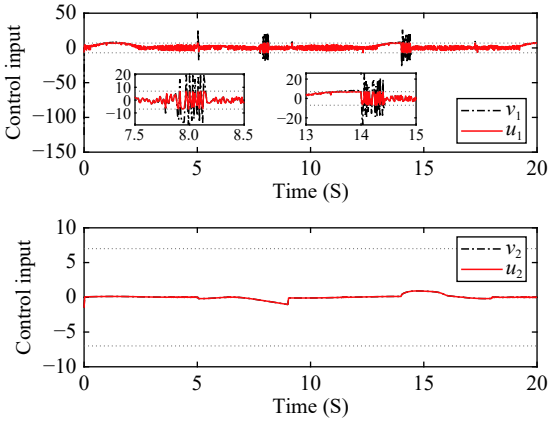

Figure 9. Example 2: Trajectories of the saturation input u_i and v_i.

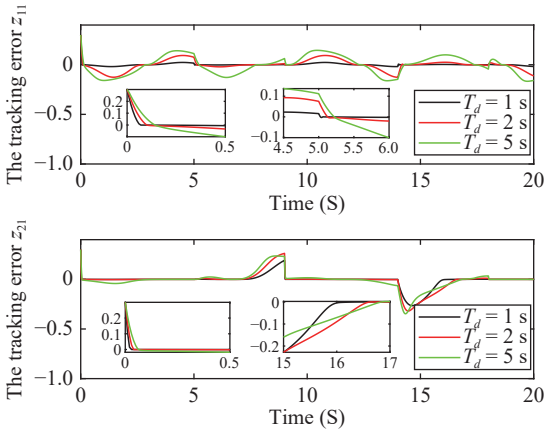

Figure 10. Example 2: Trajectories of the tracking errors z_{11} and z_{21} based on the different settling time.

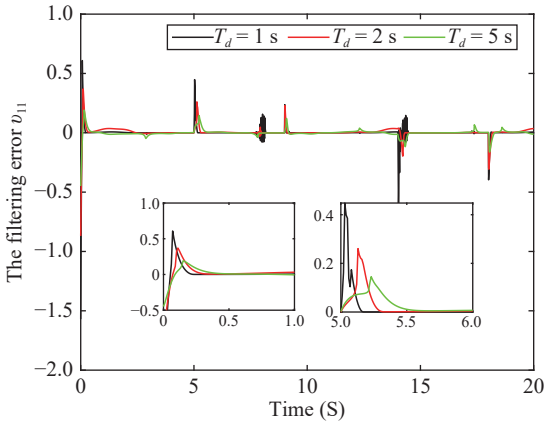

Figure 11. Example 2: Trajectories of the filtering errors v_{11} based on the different settling time.

5. Conclusion

In this article, the fuzzy adaptive predefined-time tracking control problem has been investigated for a class of switched fractional-order nonlinear systems in the presence of input saturation and external disturbances. A new predefined-time auxiliary function has been constructed to guarantee the convergence of the tracking error to a bounded compact set within a user-defined time. Furthermore, to deal with the complex calculation problem and the singularity problem, a novel predefined-time filter has been designed in the design process of an adaptive controller in order to obtain better tracking performance. In the end, the simulations have been provided to show the effectiveness of the proposed method. In the future, we will extend the proposed approach to deal with the practical prescribed-time convergence problem of the fractional-order nonlinear systems subject to cyber-attacks.

Author Contributions: All authors contributed to the study conception and design. Material preparation, data collection and analysis were performed by Lusong Ding and Weiwei Sun. The first draft of the manuscript was written by Lusong Ding and all authors commented on previous versions of the manuscript. All authors read and approved the final manuscript.

Funding: This work was supported in part by the National Natural Science Foundation of China under Grant 62073189 and Grant 62173207, in part by the Taishan Scholar Project of Shandong Province under Grant tsqn 202211129.

Conflicts of Interest: The authors declare no conflict of interest.

References

1. Bataghva, M.; Hashemi, M. Adaptive sliding mode synchronisation for fractional-order non-linear systems in the presence of time-varying actuator faults. *IET Control Theory Appl*. 2018, *12*, 377–383. doi:10.1049/iet-cta.2017.0458
2. Aghababa, M.P. Design of a chatter-free terminal sliding mode controller for nonlinear fractional-order dynamical systems. Int. J.

Control, **2013**, *86*: 1744−1756. doi: 10.1080/00207179.2013.796068
3. Nikdel, N.; Badamchizadeh, M.; Azimirad, V.; *et al*. Fractional-order adaptive backstepping control of robotic manipulators in the presence of model uncertainties and external disturbances. IEEE Trans. Ind. Electron., **2016**, *63*: 6249−6256. doi: 10.1109/TIE.2016.2577624
4. Ma, Z.Y.; Ma, H.J. Adaptive fuzzy backstepping dynamic surface control of strict-feedback fractional-order uncertain nonlinear systems. IEEE Trans. Fuzzy Syst., **2020**, *28*: 122−133. doi: 10.1109/TFUZZ.2019.2900602
5. Liu, H.; Pan, Y.P.; Li, S.G.; *et al*. Adaptive fuzzy backstepping control of fractional-order nonlinear systems. IEEE Trans. Syst. Man Cybern. Syst., **2017**, *47*: 2209−2217. doi: 10.1109/TSMC.2016.2640950
6. Jafari, A.A.; Mohammadi, S.M.A.; Farsangi, M.M.; *et al*. Observer-based fractional-order adaptive type-2 fuzzy backstepping control of uncertain nonlinear MIMO systems with unknown dead-zone. Nonlinear Dyn., **2019**, *95*: 3249−3274. doi: 10.1007/s11071-018-04754-0
7. Zhan, Y.L.; Li, X.M.; Tong, S.C. Observer-based decentralized control for non-strict-feedback fractional-order nonlinear large-scale systems with unknown dead zones. IEEE Trans. Neural Netw. Learn. Syst., **2023**, *34*: 7479−7490. doi: 10.1109/TNNLS.2022.3143901
8. Gong, P.; Lan, W.Y. Adaptive robust tracking control for multiple unknown fractional-order nonlinear systems. IEEE Trans. Cybern., **2019**, *49*: 1365−1376. doi: 10.1109/TCYB.2018.2801345
9. Sun, W.W.; Wang, L.P.; Wu, Y. Adaptive dynamic surface fuzzy control for state constrained time-delay nonlinear nonstrict feedback systems with unknown control directions. IEEE Trans. Syst. Man Cybern. Syst., **2021**, *51*: 7423−7434. doi: 10.1109/TSMC.2020.2969289
10. Sun, W.W.; Wu, Y.; Lv, X.Y. Adaptive neural network control for full-state constrained robotic manipulator with actuator saturation and time-varying delays. IEEE Trans. Neural Netw. Learn. Syst., **2022**, *33*: 3331−3342. doi: 10.1109/TNNLS.2021.3051946
11. Ding, D.R.; Wang, Z.D.; Han, Q.L. Neural-network-based consensus control for multiagent systems with input constraints: The event-triggered case. IEEE Trans. Cybern., **2020**, *50*: 3719−3730. doi: 10.1109/TCYB.2019.2927471
12. Wen, C.Y.; Zhou, J.; Liu, Z.T.; *et al*. Robust adaptive control of uncertain nonlinear systems in the presence of input saturation and external disturbance. IEEE Trans. Automat. Control, **2011**, *56*: 1672−1678. doi: 10.1109/TAC.2011.2122730
13. Chen, M.; Ge, S.S.; Ren, B.B. Adaptive tracking control of uncertain MIMO nonlinear systems with input constraints. Automatica, **2011**, *47*: 452−465. doi: 10.1016/j.automatica.2011.01.025
14. Song, S.; Zhang, B.Y.; Song, X.N.; *et al*. Neuro-fuzzy-based adaptive dynamic surface control for fractional-order nonlinear strict-feedback systems with input constraint. IEEE Trans. Syst. Man Cybern. Syst., **2021**, *51*: 3575−3586. doi: 10.1109/TSMC.2019.2933359
15. Wang, C.H.; Cui, L.M.; Liang, M.; *et al*. Adaptive neural network control for a class of fractional-order nonstrict-feedback nonlinear systems with full-state constraints and input saturation. IEEE Trans. Neural Netw. Learn. Syst., **2022**, *33*: 6677−6689. doi: 10.1109/TNNLS.2021.3082984
16. Cao, B.Q.; Nie, X.B. Event-triggered adaptive neural networks control for fractional-order nonstrict-feedback nonlinear systems with unmodeled dynamics and input saturation. Neural Netw., **2021**, *142*: 288−302. doi: 10.1016/j.neunet.2021.05.014
17. Zeng, D.P.; Liu, Z.; Chen, C.L.P.; *et al*. Event-triggered fuzzy adaptive control of nonlinear switched systems with predefined accuracy and mismatched switching. Fuzzy Sets Syst., **2022**, *443*: 283−307. doi: 10.1016/j.fss.2021.10.004
18. Geng, H.; Wang, Z.D.; Yi, X.J.; *et al*. Tobit Kalman filtering for fractional-order systems with stochastic nonlinearities under round-robin protocol. Int. J. Robust Nonlinear Control, **2021**, *31*: 2348−2370. doi: 10.1002/rnc.5396
19. Sisbot, E.A.; Marin-Urias, L.F.; Alami, R.; *et al*. A human aware mobile robot motion planner. IEEE Trans. Robot., **2007**, *23*: 874−883. doi: 10.1109/TRO.2007.904911
20. Shi, K.B.; Wang, J.; Zhong, S.M.; *et al*. New reliable nonuniform sampling control for uncertain chaotic neural networks under Markov switching topologies. Appl. Math. Comput., **2019**, *347*: 169−193. doi: 10.1016/j.amc.2018.11.011
21. Ma, R.C.; Zhao, J. Backstepping design for global stabilization of switched nonlinear systems in lower triangular form under arbitrary switchings. Automatica, **2010**, *46*: 1819−1823. doi: 10.1016/j.automatica.2010.06.050
22. Long, L.J.; Zhao, J. Switched-observer-based adaptive neural control of MIMO switched nonlinear systems with unknown control gains. IEEE Trans. Neural Netw. Learn. Syst., **2017**, *28*: 1696−1709. doi: 10.1109/TNNLS.2016.2521425
23. Bi, W.S.; Wang, T.; Yu, X.H. Fuzzy adaptive decentralized control for nonstrict-feedback large-scale switched fractional-order nonlinear systems. IEEE Trans. Cybern., **2022**, *52*: 8887−8896. doi: 10.1109/TCYB.2021.3061136
24. Sui, S.; Chen, C.L.P.; Tong, S.C. Neural-network-based adaptive DSC design for switched fractional-order nonlinear systems. IEEE Trans. Neural Netw. Learn. Syst., **2021**, *32*: 4703−4712. doi: 10.1109/TNNLS.2020.3027339
25. Sui, S.; Tong, S.C. FTC design for switched fractional-order nonlinear systems: An application in a permanent magnet synchronous motor system. IEEE Trans. Cybern., **2023**, *53*: 2506−2515. doi: 10.1109/TCYB.2021.3123377
26. Bhat, S.P.; Bernstein, D.S. Finite-time stability of continuous autonomous systems. SIAM J. Control Optim., **2000**, *38*: 751−766. doi: 10.1137/S0363012997321358
27. Li, H.L.; Hu, C.; Zhang, L.; *et al*. Complete and finite-time synchronization of fractional-order fuzzy neural networks via nonlinear feedback control. Fuzzy Sets Syst., **2022**, *443*: 50−69. doi: 10.1016/j.fss.2021.11.004
28. Bigdeli, N.; Ziazi, H.A. Finite-time fractional-order adaptive intelligent backstepping sliding mode control of uncertain fractional-order chaotic systems. J. Franklin Inst., **2017**, *354*: 160−183. doi: 10.1016/j.jfranklin.2016.10.004
29. Kamal, S.; Raman, A.; Bandyopadhyay, B. Finite-time stabilization of fractional order uncertain chain of integrator: An integral sliding mode approach. IEEE Trans. Automat. Control, **2013**, *58*: 1597−1602. doi: 10.1109/TAC.2012.2228051
30. Polyakov, A. Nonlinear feedback design for fixed-time stabilization of linear control systems. IEEE Trans. Automat. Control, **2012**, *57*: 2106−2110. doi: 10.1109/TAC.2011.2179869
31. Sun, Y.M.; Zhang, L. Fixed-time adaptive fuzzy control for uncertain strict feedback switched systems. Inf. Sci., **2021**, *546*: 742−752. doi: 10.1016/j.ins.2020.08.059
32. Balamash, A.S.; Bettayeb, M.; Djennoune, S.; *et al*. Fixed-time terminal synergetic observer for synchronization of fractional-order chaotic systems. Chaos, **2020**, *30*: 073124. doi: 10.1063/1.5142989
33. Jiménez-Rodríguez, E.; Munoz-Vazquez, A.J.; Sanchez-Torres, J.D.; *et al*. A Lyapunov-like characterization of predefined-time stability. IEEE Trans. Automat. Control, **2020**, *65*: 4922−4927. doi: 10.1109/TAC.2020.2967555
34. Munoz-Vazquez, A.J.; Sánchez-Torres, J.D.; Jiménez-Rodríguez, E.; *et al*. Predefined-time robust stabilization of robotic manipulators. *IEEE/ASME Trans. Mechatron*. **2019**, *24*, 1033–1040. doi:10.1109/TMECH.2019.2906289

35. Zhang, T.L.; Bai, R.; Li, Y.M. Practically predefined-time adaptive fuzzy quantized control for nonlinear stochastic systems with actuator dead zone. IEEE Trans. Fuzzy Syst., **2023**, *31*: 1240−1253. doi: 10.1109/TFUZZ.2022.3197970
36. Wang, Q.; Cao, J.D.; Liu, H. Adaptive fuzzy control of nonlinear systems with predefined time and accuracy. IEEE Trans. Fuzzy Syst., **2022**, *30*: 5152−5165. doi: 10.1109/TFUZZ.2022.3169852
37. Yang, T.T.; Dong, J.X. Predefined-time adaptive fault-tolerant control for switched odd-rational-power multi-agent systems. IEEE Trans. Autom. Sci. Eng., **2023**, *20*: 2423−2434. doi: 10.1109/TASE.2022.3208029
38. Xu, H.; Yu, D.X.; Sui, S.; *et al*. An event-triggered predefined time decentralized output feedback fuzzy adaptive control method for interconnected systems. IEEE Trans. Fuzzy Syst., **2023**, *31*: 631−644. doi: 10.1109/TFUZZ.2022.3184834
39. Yu, Z.L.; Li, Y.H.; Lv, M.L.; *et al*. Predefined-time anti-saturation fault-tolerant attitude control for tailless aircraft with guaranteed output constraints. Nonlinear Dyn., **2023**, *111*: 1399−1416. doi: 10.1007/s11071-022-07904-7
40. Xu, K.T.; Ge, M.F.; Liang, C.D.; *et al*. Predefined-time time-varying formation control of networked autonomous surface vehicles: A velocity- and model-free approach. Nonlinear Dyn., **2022**, *108*: 3605−3622. doi: 10.1007/s11071-022-07415-5
41. Xie, S.Z.; Chen, Q.; He, X.X. Predefined-time approximation-free attitude constraint control of rigid spacecraft. IEEE Trans. Aerosp. Electron. Syst., **2023**, *59*: 347−358. doi: 10.1109/TAES.2022.3183550
42. Muñoz-Vázquez, A.J.; Sánchez-Torres, J.D.; Defoort, M.; *et al*. Predefined-time convergence in fractional-order systems. Chaos Solitons Fractals, **2021**, *143*: 110571. doi: 10.1016/j.chaos.2020.110571
43. Muñoz-Vázquez, A.J.; Sánchez-Torres, J.D.; Defoort, M. Second-order predefined-time sliding-mode control of fractional-order systems. Asian J. Control, **2022**, *24*: 74−82. doi: 10.1002/asjc.2447
44. Cui, M.Y.; Tong, S.C. Event-triggered predefined-time output feedback control for fractional-order nonlinear systems with input saturation. *IEEE Trans. Fuzzy Syst*. **2023**, in press. doi:10.1109/TFUZZ.2023.3283783
45. Podlubny, I. *Fractional Differential Equations*; Academic Press: San Diego, CA, USA, 1999.
46. Li, C.P.; Deng, W.H. Remarks on fractional derivatives. Appl. Math. Comput., **2007**, *187*: 777−784. doi: 10.1016/j.amc.2006.08.163
47. Aguila-Camacho, N.; Duarte-Mermoud, M.A.; Gallegos, J.A. Lyapunov functions for fractional order systems. Commun. Nonlinear Sci. Numer. Simul., **2014**, *19*: 2951−2957. doi: 10.1016/j.cnsns.2014.01.022
48. Wang, L.X.; Mendel, J.M. Fuzzy basis functions, universal approximation, and orthogonal least-squares learning. IEEE Trans. Neural Netw., **1992**, *3*: 807−814. doi: 10.1109/72.159070
49. Mani, P.; Rajan, R.; Shanmugam, L.; *et al*. Adaptive fractional fuzzy integral sliding mode control for PMSM model. IEEE Trans. Fuzzy Syst., **2019**, *27*: 1674−1686. doi: 10.1109/TFUZZ.2018.2886169

Citation: Ding, L.; Sun, W. Predefined Time Fuzzy Adaptive Control of Switched Fractional-Order Nonlinear Systems with Input Saturation. *International Journal of Network Dynamics and Intelligence*. 2023, 2(4), 100019. doi: 10.53941/ijndi.2023.100019